Light-driven optimisation of high-value aromatic compound production in metabolically engineered cyanobacteria

Bioresource Technology Reports 31 (2025) 102216

Contents lists available at ScienceDirect

Bioresource Technology Reports

journal homepage: www.sciencedirect.com/journal/bioresource-technology-reports

Light-driven optimisation of high-value aromatic compound production in metabolically engineered cyanobacteria

Giulia Usai [a,b,*], Nicolò Santi Vasile [a,c], Davide Scabello [a,b], Elena Mazzocchi [a,b], Debora Fino [b], Candido Fabrizio Pirri [a,b], Barbara Menin [a,d], Alessandro Cordara [a,c,**]

[a] Centre for Sustainable Future Technologies, Fondazione Istituto Italiano di Tecnologia, Via Livorno, 60, 10144 Turin, Italy
[b] Department of Applied Science and Technology—DISAT, Politecnico di Torino, Corso Duca degli Abruzzi, 24, 10129 Turin, Italy
[c] Department of Environment, Land and Infrastructure Engineering—DIATI, Politecnico di Torino, Corso Duca degli Abruzzi, 24, 10129 Turin, Italy
[d] Istituto di Biologia e Biotecnologia Agraria, Consiglio Nazionale delle Ricerche IBBA-CNR, Via Alfonso Corti 12, 20133 Milan, Italy

ARTICLE INFO

Keywords:
Cyanobacteria
CO_2
Photosynthetic microbial factories
Bioprocesses
2-Phenylethanol
Photobioreactors
3-D light modelling

ABSTRACT

The development of a circular, bio-based economy is a major challenge of this century. Photosynthesis-driven biomanufacturing offers a sustainable approach to biotechnological production and CO_2 recycling, contributing to carbon neutrality. This study examines the effect of different light intensities on the metabolically engineered cyanobacterium *Synechococcus elongatus* PCC 7942 (2PE_*aroK* strain), which produces 2-phenylethanol (2-PE), a valuable aromatic compound used in food and cosmetics industries. The investigation was conducted in a flat-panel photobioreactor under various light conditions (0–500 µmol photons m^{-2} s^{-1}). We identified 150 µmol photons m^{-2} s^{-1} as optimal, yielding 282 mg L^{-1} 2-PE, with a productivity of 28.7 mg L^{-1} d^{-1} and 87 % light absorption efficiency. At lower light intensities, 45–50 % of carbon was allocated to 2-PE, decreasing to 28 % at higher intensity. The study highlights the metabolic interplay between photosynthesis, carbon utilisation, and target product formation, providing insights for optimised photosynthesis-based biomanufacturing.

1. Introduction

Photosynthesis-driven bioprocessing represents a promising avenue for sustainable biotechnology, offering applications ranging from renewable energy to high-value compounds. By utilising light and carbon dioxide (CO_2) as primary inputs, photosynthetic microorganisms such as microalgae and cyanobacteria provide a renewable solution to industrial manufacturing, contributing significantly to efforts to limit greenhouse gas emissions and achieve carbon neutrality (Hamouda and El-Ahmady El-Naggar, 2021; Levasseur et al., 2020). These microbe-based solutions provide a renewable approach to biomanufacturing, aligning with global efforts to limit climate change.

Among photosynthetic organisms, prokaryotic cyanobacteria stand out as particularly promising candidates for industrial applications. They possess highly efficient oxygenic photosynthesis, exhibit rapid growth, reach high cell densities (Schuurmans et al., 2015) and are amenable to genetic modification (Berla et al., 2013). Despite their potential, the transition from laboratory-scale research to commercial-scale production is fraught with challenges, including strain selection, optimisation of cultivation conditions, and scaling up in photobioreactors (PBRs). Among the many factors affecting microalgae biotechnology (e.g. temperature, pH, carbon source, mixing) light is dominant. Light serves as the primary energy source for photosynthesis, directly driving cellular metabolism and growth. The role of light in photosynthetic efficiency and biotechnological production has been extensively studied (Kwan et al., 2021; Lisondro et al., 2022; Rahman et al., 2023). Both natural and artificial light sources are employed for photosynthetic cultivation. Open systems, such as raceway ponds, often rely on sunlight, while closed systems, such as photobioreactors, utilise artificial lighting due to its precise controllability. Artificial light can be modulated to enhance both biomass and product yields, making it a preferred option for high-value compound production. Additionally, several strategies are being developed to improve the economic feasibility of artificial light systems in large-scale photosynthetic production.

* Corresponding author at: Fondazione Istituto Italiano di Tecnologia, Via Livorno, 60, 10144 Turin, Italy.
** Correspondence to: A. Cordara, Politecnico di Torino, Corso Duca degli Abruzzi, 24, 10129 Turin, Italy.
E-mail addresses: giulia.usai@iit.it (G. Usai), nicolo.vasile@polito.it (N.S. Vasile), davide.scabello@iit.it (D. Scabello), elena.mazzocchi@iit.it (E. Mazzocchi), debora.fino@polito.it (D. Fino), fabrizio.pirri@iit.it (C.F. Pirri), barbara.menin@ibba.cnr.it (B. Menin), alessandro.cordara@polito.it (A. Cordara).

https://doi.org/10.1016/j.biteb.2025.102216
Received 20 December 2024; Received in revised form 8 July 2025; Accepted 9 July 2025
Available online 14 July 2025

These include optimizing reactor designs to improved light distribution (Do et al., 2022), applying tailored light spectra (Luimstra et al., 2018), and integrating renewable energy sources or natural sunlight (Sforza et al., 2015) to reduce operational costs and environmental impact. Therefore, the energy cost for light should be evaluated, since it largely influences the price of compounds produced by microalgae-driven factories (Maltsev et al., 2021). Among all the light sources, e.g. tungsten, fluorescent, halogen, high-pressure sodium lamps, it has been estimated that 15–16 US$ kg^{-1} can be spent for light-emitting diodes (LEDs) illumination system, largely adopted nowadays (Blanken et al., 2013; Singh and Mishra, 2023). Additionally, artificial lighting is not subject to geographic or seasonal variations, allowing for year-round biomanufacturing. While more expensive, artificial lighting typically results in greater biomass and product yields compared to natural illumination, improving the overall efficiency of biomanufacturing processes (Sobolewska et al., 2023; Kratky et al., 2023). Noteworthy, using artificial light allows to set several parameters, such as photon flux, light-dark cycles, and spectral composition to address specific tasks for specific strains.

In this regard, to better align with physiological requirements of microalgae or cyanobacteria for optimal biomanufacturing, systematic studies are needed to find the exact light delivery to achieve resource utilisation efficiency and sustainability. Inevitably, concerns about how light and the resulting photosynthesis rate affect the productivity of target compounds need to be addressed by unveiling the kinetic features of the ongoing bioproduction. Generally, under varying light regimes and cycle, microorganisms dynamically adjust the allocation of energy carriers (e.g., ATP, NADPH) and carbon precursors to balance biomass growth and metabolite production (Jaiswal and Wangikar, 2020). High light intensities typically increase the flux through the Calvin–Benson–Bassham (CBB) cycle and downstream biosynthetic pathways, potentially enhancing the activity of key metabolic enzymes via transcriptional mechanisms (e.g. RpaB, LexA) (Hanaoka et al., 2012; Oliveira and Lindblad, 2011). Previous studies have explored these regulatory responses under different light conditions, but the kinetic consequences on heterologous product synthesis need to be finely studied and analysed. Therefore, bioprocess engineering often faces challenges, such as competition between biomass production and the formation of the desired heterologous product, since both rely on shared metabolic precursors. Additionally, carbon sinks introduced into wild-type or engineered strains can cause redox imbalances, potentially reducing overall productivity (Du et al., 2018b; Branco Dos Santos et al., 2014). Thus, cells often activate side pathways to meet their metabolic needs and correct this imbalance (Nogales et al., 2012). One strategy to address this issue involves the deletion of those enzymes/pathways that interfere with the target production. However, this approach can compromise the cell fitness, resulting in a weaker microorganism (Nogales et al., 2012), especially if designated for industrial application where robustness is essential. Furthermore, integrating experimental data with advanced bioprocess modelling can provide insights into the complex interplay of factors affecting productivity. Computational tools that simulate light diffusion, mass transfer, and growth kinetics in photobioreactors offer valuable guidance for designing efficient and scalable processes.

This study investigates the impact of light intensity on the heterologous production of 2-phenylethanol (2-PE) by an engineered cyanobacterial strain, *Synechococcus elongatus* PCC 7942 (2PE_*aroK*) (Usai et al., 2022). 2PE_*aroK* mutants overexpresses five key enzymes (see Table 1 for more details, Fig. 1) involved in the shikimate pathway, the primary route for aromatic compound synthesis (Mir et al., 2015). Those enzymes -DAHP synthase (*aroG*^{fbr}), shikimate kinase (*aroK*), chorismate mutase/prephenate dehydratase (*pheA*^{fbr}), phenylpyruvate decarboxylase (*kivD*) and alcohol dehydrogenase A (*adhA*)- work together to produce 2-PE, a high-value aromatic alcohol with applications in the fragrance and food industries, with pleasant rose flavour (Etschmann et al., 2002; Fang and Sung, 2021; Drężek et al., 2024). Additionally, the increasing demand for natural and biological products are contributing enormously to push scientific efforts towards high-value marketable aromatic compounds, e.g. 2-PE (Dickey et al., 2024). In this panorama, the biotechnological production should reduce costs significantly to approximately 220 USD/kg (Martínez-Avila et al., 2018), making it a promising alternative to the most common chemical synthesis and plant extraction.

Here, to explore the light-dependent kinetics of 2-PE production, we cultivated the 2PE_*aroK* strain in a flat-panel photobioreactor under five light conditions (0, 100, 150, 300, and 500 μmol photons m^{-2} s^{-1}) during two-stage batch cultivation. Carbon allocation between biomass and 2-PE was quantified, elucidating the trade-offs involved in light utilisation efficiency. In addition, we compared the optimal light condition identified during batch cultivation with semi-continuous cultivation. Also, we implemented a 3D multiphysics mathematical model of a flat-panel PBR (Vasile et al., 2021), including phenomena such as fluid dynamics, growth kinetics, mass transfer, and light diffusion, to describe the current bioprocess. Despite previous literature (Usai et al., 2022, 2024), we significantly improved 2-PE productivity in the 2PE_aroK strain by identifying and optimising key parameters and elucidating their interactions within the biosystem. By addressing the interplay between light delivery, photosynthetic efficiency, and target compound synthesis, this study provides critical insights into resource allocation in engineered cyanobacteria. Our findings contribute to the rational design of photosynthetic bioprocesses, offering comprehensive strategies to optimise light utilisation and reduce energy costs in sustainable biomanufacturing platforms for high-value aromatic compounds.

2. Materials and methods

2.1. Cyanobacteria inoculum preparation for PBR

The entire set of experiments was conducted using the recombinant strain of *Synechococcus elongatus* PCC 7942, called 2PE_*aroK*, which was

Table 1
Genetic features of 2PE_aroK recombinant strain of *S. elongatus* PCC 7942. HR, homologous recombination; NS, neutral site; DAHP, 3-deoxy-7-phosphoheptulonate; PEP, phosphoenolpyruvate; E4P, erythrose-4-phosphate.

Gene	HR Site	Protein	EC number	Reaction	Organism	Ref.
aroG^{fbr}	NSI	Feedback-inhibition resistant DAHP synthase	EC 2.5.1.54	PEP + E4P + H_2O ⇌ DAHP + Pi	*Escherichia coli*	(Ni et al., 2018; Usai et al., 2022)
pheA^{fbr}	NSI	Feedback-inhibition resistant chorismate mutase/prephenate dehydratase	EC 5.4.99.5/EC 4.2.1.51	Chorismate ⇌ Prephenate ⇌ Phenylpyruvate + H_2O + CO_2	*Escherichia coli*	(Ni et al., 2018; Usai et al., 2022)
kivD	NSI	Phenylpyruvate decarboxylase	EC 4.1.1.43	Phenylpyruvate ⇌ Phenylacetaldehyde + CO_2	*Lactococcus lactis*	(Ni et al., 2018; Usai et al., 2022)
adhA	NSI	Alcohol dehydrogenase A	EC 1.1.1.1	Phenylacetaldehyde + NAD(*P*)H ⇌ 2-Phenylethanol + $NAD(P)^+$	*Synechocystis PCC 6803*	(Ni et al., 2018; Usai et al., 2022)
aroK	NSII	Shikimate kinase	EC 2.7.1.71	Shikimate + ATP ⇌ Shikimate-3-P + ADP	*S. elongatus PCC 7942*	(Usai et al., 2022)

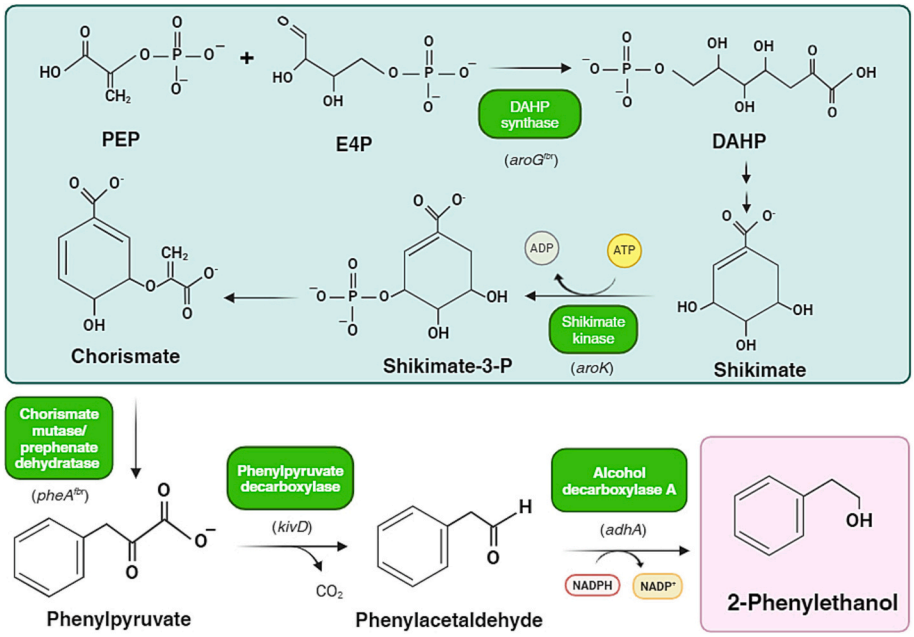

Fig. 1. Scheme of the pathway for 2-PE biosynthesis in 2PE_aroK mutant strain. All the overexpressed proteins are labelled in green. The blue box includes all the reactions taking part of the shikimate pathway. PEP, phosphoenolpyruvate; E4P, erythrose-4-phosphate; DAHP, 3-deoxy-D-arabino-heptulosonic acid 7-phosphate. (For interpretation of the references to color in this figure legend, the reader is referred to the web version of this article.)

previously developed by our laboratory (Usai et al., 2022). Table 1 reports the gene and protein features that the mutant strain carries. The mutant cyanobacteria inoculum to seed the PBR were grown in Erlenmeyer flasks, at 30 °C, 130 rpm and constant illumination of 30 μmol photons m^{-2} s^{-1} (New Brunswick™ Innova® 44 Shaker). The culture were grown in BG11 medium, following the recipe as described: 1.5 g L^{-1} $NaNO_3$, 0.075 g L^{-1} $MgSO_4{\cdot}7H_2O$, 0.004 g L^{-1} $FeCl_3{\cdot}6H_2O$, 0.04 g L^{-1} K_2HPO_4, 0.036 g L^{-1} $CaCl_2$, 0.024 g L^{-1} $Na_2EDTA{\cdot}2H_2O$, 2.86 g L^{-1} H_3BO_3, 1.81 mg L^{-1} $MnCl_2{\cdot}4H_2O$, 0.39 mg L^{-1} $Na_2MoO_4{\cdot}2H_2O$, 0.22 mg L^{-1} $ZnSO_4{\cdot}7H_2O$, mg L^{-1} $CuSO_4{\cdot}5H_2O$, and mg L^{-1} $Co(NO_3)_2{\cdot}6H_2O$. The BG11 medium was buffered with 6.05 g L^{-1} TES (2-([Tris(hydroxymethyl)methyl]amino)ethane-1-sulfonic acid sodium salt) to pH = 8. The BG11 medium was supplemented with 20 μg mL^{-1} spectinomycin and 10 μg mL^{-1} kanamycin.

2.2. Experimental design in flat-panel PBR

2PE_*aroK* recombinant strain was studied in flat panel PBR system, i.e. the FMT150.2/400 (Photon Systems Instruments, Drasov, Czech Republic) (Nedbal et al., 2008), equipped with a customised vessel of 450 mL of working volume. All the geometrical parameters were thoroughly illustrated in Vasile et al. (2021). Cyanobacteria were grown in the BG11 medium as described above but supplemented with 10 mM of $NaHCO_3$ as buffering system. The optical density (OD) was constantly measured by an integrated densitometer at 720 and 680 nm. The PBR is equipped with a probe for temperature and pH. The temperature was settled at 30 ± 1 °C and pH = 8. A constant supply of CO_2 was provided by sparging the medium with 1 % CO_2 (v/v) in N_2. A gas mixer (GMS150 micro, Photon Systems Instruments, Drásov, Czech Republic) coupled to a mass flow controller (EL-FLOW prestige FG-201CV, Bronkhorst High-Tech BV, AK Ruurlo, Netherland) to supply 150 mL min^{-1} of gas mixture to the PBR. The cyanobacteria cultures were illuminated with white light from one side of the PBR by LEDs.

For the liquid batch experiments, all tests were conducted following two stages: i) growth phase, the cells were gradually acclimated to the increasing light up to the chosen one, until the culture reached OD_{730} = 1; and ii) production phase, triggered by adding to the mutant culture (OD_{730} = 1) 1 mM IPTG and 0.3 g L^{-1} L-Phe, as gene expression inducer and metabolite doper, respectively. During the second stage, characterised by the induction of 2-PE synthesis pathway, the light was kept constant at 0, 100, 150, 300 or 500 μmol photons m^{-2} s^{-1} and this phase was preceded by an acclimation of 24–48 h at the target light. The OD was daily monitored at 730 nm and converted in biomass as g of dry cell weight per L of culture (g DW L^{-1}), by using the conversion factor of 0.26 previously determined in our laboratory.

The PBR was run in turbidostat (semicontinuous) mode by a controlled dilution of the growing cell population. Dilution was based on the changes at OD_{720}, measured by the integrated densitometer and calibrated to the benchtop spectrometer at OD_{730} to maintain the OD_{730} approximately at 1 ± 3 %, keeping the culture in exponential phase. The turbidostat mode followed the same experimental set up described above. Firstly, the biomass was accumulated in batch mode until the cyanobacteria culture reached OD_{730} = 1, then the turbidostat mode was activated. The cell culture was subjected to 24–48 h of turbidostat at 150 μmol photons m^{-2} s^{-1}, to acclimate the cells to both light and cultivation mode. To lunch the production phase 1 mM IPTG and 0.3 g L^{-1} L-Phe was directly supplemented into the vessel as well as into the BG11 medium for the controlled dilution, to avoid the washout of the gene expression inducer and the metabolite doper. Dilution was performed by a peristaltic pump automatically controlled by the software of the photobioreactor, accordingly to the selected OD_{720} range.

2.3. Light transmission modelling in flat-panel PBR

The 3D multi-physics, multi-component, multi-phase, and not isothermal model of the flat-panel PBR was developed on the COMSOL 6® platform, previously in our laboratory (Cordara et al., 2018; Vasile et al., 2021). Briefly, the model simulates the several phenomena, i.e. heat transfer and radiation in different media, bacterial growth kinetics, transport of species, fluid dynamic with gas-liquid mass transfer and particle tracing by providing the corresponding equations (Li et al., 2014). Additionally, the design of the 3D model based on the PBR geometry accounts for the presence of the glass and probes for CO_2 and pH inside the liquid mixture (Supplementary Fig. S1) and their effect on light transmission (Vasile et al., 2021; Tamburic et al., 2018). The light distribution within the reactor was modelled using the Discrete

Ordinates Method, which allows for detailed calculations of radiative transfer across different domains of the photobioreactor at various time intervals. This method solves the radiative transfer equation (RTE) for a finite number of discrete directions, capturing the anisotropic scattering and absorption of light by the cyanobacterial cells and gas bubbles within the culture medium. Additionally, the model adapts Lambert-Beer's law to account for the presence of bubbles and cells (Zhang et al., 2015), and the modified Monod equation to describe the growth kinetics of cyanobacteria, incorporating the effects of nutrient concentration and light intensity on the maximum specific growth rate (Zhang et al., 2015; Dechatiwongse et al., 2014). The adaptation of Lambert-Beer's law was validated experimentally following the procedure described in previous work (Vasile et al., 2021), by comparing measured and simulated outlet transmitted light through the photobioreactor in both abiotic and biotic conditions. As shown in Supplementary Fig. S5, the excellent agreement confirms the model's accuracy in reproducing light distribution across different biomass concentrations and photon fluxes. Parameters for the growth model and the light transmission were fitted using experimental data, employing a combination of the Levenberg-Marquardt method and second least-squares analysis to ensure the model's parameters accurately reflect observed growth dynamics (Cordara et al., 2018). For fluid-dynamics and particle tracking algorithms were employed to simulate the trajectories and light exposure of individual cyanobacterial cells (Li et al., 2014; Luo and Al-Dahhan, 2011). Additionally, the reactor geometry was precisely reproduced using free tetrahedral meshing, selected to ensure the accuracy and precision of the simulation results. All the equations employed in the model can be found in Supplementary Table S1.

2.4. qRT-PCR analysis

qRT-PCR analysis was performed as described in Usai et al. (2022). All the primers used are reported in Supplementary Table S2. The expression levels of the target genes (*kivD*, *adhA*, *aroG*^{fbr}, *pheA*^{fbr}, *aroK*) were relatively quantified against the reference *prs* gene (Usai et al., 2022; Luo et al., 2019) by the Pfaffl method (Mannino et al., 2021), using the gene expression level at the lowest light intensity as control condition. The analysis was conducted from the biomass harvested five days after the induction of the gene expression.

2.5. CO_2 consumption

To measure the dissolved CO_2 (dC) into the cultural medium, the PBR was equipped with the CO_2 sensor InPro 5000/12/120 (Mettler Toledo, Columbus, Ohio, United States), based on the Severinghaus principle (Severinghaus and Bradley, 1958). Briefly, the electrode contains sodium bicarbonate, which reacts with the CO_2. The reaction changes the pH in the electrode, which corresponds to a change in potential difference, and this is measured. Therefore, the CO_2 is then inferred by changes in pH every minute. Furthermore, the dissolved CO_2 values were used to experimentally calculate the kLa, the volumetric mass transfer coefficient, under abiotic PBR condition. The CO_2 liquid transfer is represented by an exponential curve until a plateau, which represent the saturation limit (dC_{sat}) under the settled PBR condition. Thus, the CO_2 transfer rate (CTR) was determined from the measured dissolved CO_2 values (dC_n), as follows (Eq. a):

$$CTR = \Delta dC \Big/ \Delta t = \ln\left(\frac{dC_{sat} - dC_n}{dC_{sat} - dC_{n+1}}\right) \quad (a)$$

Being aware of the CTR every minute, the kLa values were calculated within the exponential phase of the dissolution curve and the resulting value was the average of those calculated (Eq. b):

$$kLa = CTR/dC_n \quad (b)$$

The resulting kLa was then used for calculating the CO_2 uptake by bacteria. First the theoretical dissolved CO_2 value (dCc) was calculated as follows (Eq. c):

$$dC_c = dC_{sat} - \left(\frac{dC_{sat} - dC_n}{\exp(kLa^{*}\Delta t)}\right) \quad (c)$$

Finally, the CO_2 uptake was calculated every minute as (Eq. d):

$$C\ uptake = dC_c - dC_n \quad (d)$$

2.6. Analytics

2-PE and L-phenylalanine were quantified by HPLC as reported in Usai et al. (2022, 2024). For the carbohydrate quantification as glycogen, 1 mL of cell culture was collected before and after the induction of gene expression. The cell cultures were centrifuged at 12,000 *g* for 10 min and processed as previously reported in Brey et al. (2020).

2.7. Carbon balance

To determine the carbon distribution, the carbon balance was calculated considering together the two carbon sources, i.e. CO_2 and L-Phe, used to produce biomass and 2-PE. Each C source consumed and product synthesised was converted to the corresponding moles of carbon atoms. In the case of biomass, the carbon content of *S. elongatus* PCC 7942 biomass corresponds to approximately 46–48 % of its dry weight (Mahlmann et al., 2008). Thus, the carbon balance was calculated for both the biomass (Eq. e) and 2-PE (Eq. f):

$$C_{biomass} = \frac{Cmol\ biomass}{(Cmol\ CO_2 + Cmol\ L - Phe)}{}^{*}100 \quad (e)$$

$$C_{2-PE} = \frac{Cmol\ 2 - PE}{(Cmol\ CO_2 + Cmol\ L - Phe)}{}^{*}100 \quad (f)$$

2.8. Photosynthetic pigments quantification

Phycocyanin (phy), Chlorophyll a (chla) and total carotenoids (car) were quantified in each sample. Briefly, 1 mg of dried biomass was weighted and resuspended in 1 mL of PBS solution and kept on ice. The suspension was added to a tube containing 500 mg of glass beads (0.25–0.5 mm). The lysis was performed twice in a tissue lyser (Retsch MM 400, Haan, Germany), at 15 s^{-1} for 5 min. The lysate was then incubated on ice for 1 h and then centrifuged at +4 °C, 15,000*g* for 10 min. The supernatant was opportunely diluted and used for spectrophotometric measurements (PerkinElmer Lambda 650 UV/Vis). The absorbance was collected in the range from 800 nm to 500 nm. The phycocyanin concentration was measured through the following equation (Zavřel et al., 2018):

$$\text{Phycocyanin}\left[\text{mg mL}^{-1}\right] = \left((A_{615} - A_{720}) - 0.474 \times (A_{652} - A_{720})\right)/5.34 \quad \text{(g)}$$

The remaining cell pellet was resuspended in 1 mL of cold methanol (≥99.9 %) and incubated at 4 °C in the darkness for 20 min. The cells debris were centrifuged (12,000*g*, 10 min, 4 °C) to recover the supernatant, which was properly diluted in methanol and then subjected to spectrophotometer in the range of 800 nm to 400 nm. To calculate the photosynthetic pigments concentration, the following equations were used (Wellburn, 1994):

$$\text{Chlorophyll a}\left[\mu\text{g mL}^{-1}\right] = 12.9447(A_{665} - A_{720}) \quad \text{(h)}$$

$$\text{Total carotenoids}\left[\mu\text{g mL}^{-1}\right] = \left[1000(A_{470} - A_{720}) - 2.86\left(\text{Chla}\left[\mu\text{g mL}^{-1}\right]\right)\right]/221 \quad \text{(i)}$$

The relative pigments concentrations were normalised on the basis of the biomass used for the pigments extraction and the final results were expressed as mg of pigment per gDW (mg g DW^{-1}).

2.9. Statistics

Statistical analyses were developed using GraphPad Prism software (version 10.1.2; GraphPad Software, San Diego, CA, USA). A one- or two-way ANOVA analysis was applied. Asterisks in figures indicate significance levels as follows: $p \leq 0.05$ (*), $p \leq 0.002$ (**), $p \leq 0.0002$ (***), and $p \leq 0.0001$ (****). Data are presented as mean ± standard deviation (SD), by the means of four biological replicates.

3. Results

3.1. Effect of photon fluxes on growth kinetics of 2PE_aroK mutant strain

To expand knowledge about the metabolic relationship between the light, which acts directly on photosynthesis, and the non-native pathway introduced for 2-PE production in the 2PE_*aroK* mutant strain, five different light conditions (dark, 100, 150, 300 or 500 µmol photons m^{-2} s^{-1}) were assessed. Data about cell growth, fitness, carbon consumption and 2-PE production were collected in each condition. Most of the data are related to the production phase (10–12 days), triggered by adding IPTG and L-Phe, which induce the gene expression and the metabolite doping, respectively. The production phase started when the bacterial culture reached $OD_{730} = 1$, corresponding to 0.26 g DW L^{-1}, and was exposed to the desired photon flux for at least 24 h. Table 2 reports a summary of the main experimental data obtained in this study. Unsurprisingly, both the highest biomass production (Fig. 2A, B) and specific growth rate (Fig. 2C; µ, d^{-1}) were obtained at the most intense light condition, following, however, a non-linear trend among the tested light conditions ($R^2 = 0.034$). Actually, the growth rate at the highest photon flux improved only by 19 % compared to that one at 100 µmol photons m^{-2} s^{-1}. This phenomenon can be due to a self-shading effect. During the production phase (2nd stage of the bioprocess), in almost all the light conditions tested, the biomass accumulated by 70–75 % of the total biomass production, exception for the lowest light condition, where the biomass accumulated by 58 % (Fig. 2B, blue bars). As expected, since *S. elongatus* is a known obligate photoautotrophic organism, no bacterial growth was observed during the production phase conducted in the dark (Fig. 2A), with biomass levels remaining unchanged from those achieved during the growth phase (Table 2). Additionally, qRT-PCR analysis was performed to understand whether the light intensities or the environmental conditions could affect the gene expression level. The analysis has been conducted using the lowest light intensity as calibrator and *prs* gene as reference gene as previously described (Usai et al., 2022; Luo et al., 2019), which is known to be one of the most stably expressed gene in cyanobacteria. However, no worthy-of-mention results emerged in every light exposure. Details are provided in the Supplementary Fig. S2. Overall, all the genes were expressed in every light condition, with no statistical significance among them.

3.2. Light distribution model for liquid batch mode in flat-panel PBR

Using in silico model previously developed by us for the flat-panel PBR (Vasile et al., 2021; Cordara et al., 2018), we assessed the light distribution into the cell cultures at each nominal light intensities of 100, 150, 300 and 500 µmol photons m^{-2} s^{-1}. All the data in the present section are related to the 2nd stage of the bioprocess, namely related to the production phase of 2-PE, triggered by the gene expression induction and metabolite doping. The experimental growth rates were firstly fitted by the modelled trend, showing how accurately the model simulates the bioprocess (Supplementary Fig. S3). The light transmission analysis through the model allowed to better understand how much light of that perceived by the bacteria was utilised by the cell culture itself. Noteworthy, the light transmission is influenced either by the distance from the light source, which explains the reduced photon fluxes than the nominal ones, or the cell population density. More details are provided in Supplementary Figs. S4 and S5. Indeed, the model calculates the averaged amount of light that any individual cell (considered as a particle) can absorb while moving in the liquid medium in every direction and, so, touching the PBR surface exposed to the light source. Additionally, the amount of light absorbed depends intrinsically on the absorption coefficient associated with cyanobacteria, leading to a non-linear increment in photons utilised by the cells as the light intensity increases (Vasile et al., 2021; Cordara et al., 2018). This coefficient is crucial in several equations of the model (reported in Supplementary Table S1) to simulate consistently both light transmission and distribution into the PBR while cultivating cyanobacteria (Soman and Shastri, 2015; Solimeno et al., 2015). The light absorption efficiency was calculated as ratio between absorbed light (I_a) and perceived light (I_p)

Table 2
Summary of the main results obtained from the liquid batch cultures exposed to five light conditions.

Photon flux	µ (d^{-1})		Final biomass (g DW L^{-1})		Max 2-PE titer (mg L^{-1})		Max 2-PE yield (mg g DW^{-1})		Average 2-PE productivity (mg L^{-1} d^{-1})		% L-Phe consumed	
(µmol photons m^{-2} s^{-1})	Average	SD	Average	SD	Average	SD	Average	SD	Average	SD	Average	SD
0	0	0	0.25	0.04	0	0	0	0	0	0	0	0
100	0.081	0.014	0.70	0.05	259.4	27.4	349.3	27.5	24.1	2.1	79.3	5.8
150	0.104	0.008	0.87	0.07	282.0	21.1	329.0	7.3	28.7	3.4	77.3	4.3
300	0.105	0.018	1.03	0.03	268.5	31.6	299.9	9.1	26.5	3.6	52.5	10.3
500	0.096	0.014	1.10	0.11	197.7	24.6	182.3	36.2	19.2	2.1	33.0	4.5

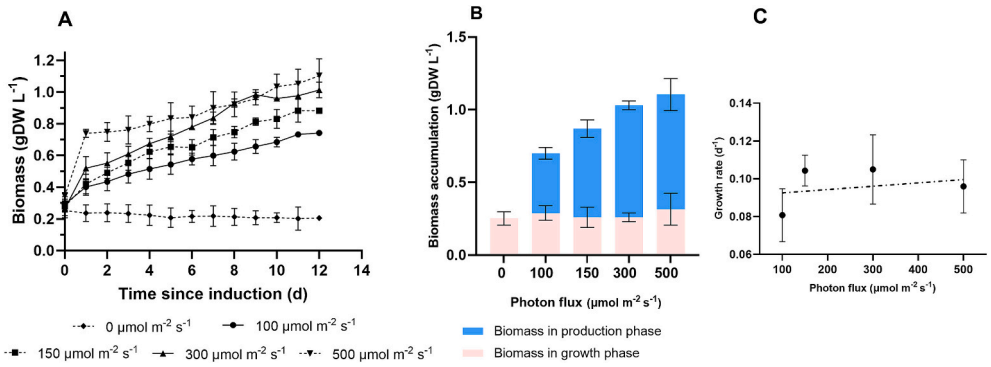

Fig. 2. 2PE_*aroK* growth data in batch cultures at four different light intensities and dark condition. A) Growth curves; B) biomass accumulation during the growth phase (pink bars) and production phase (blue bars); C) growth rates. Four biological replicates were carried out. Error bars represent standard deviation. (For interpretation of the references to color in this figure legend, the reader is referred to the web version of this article.)

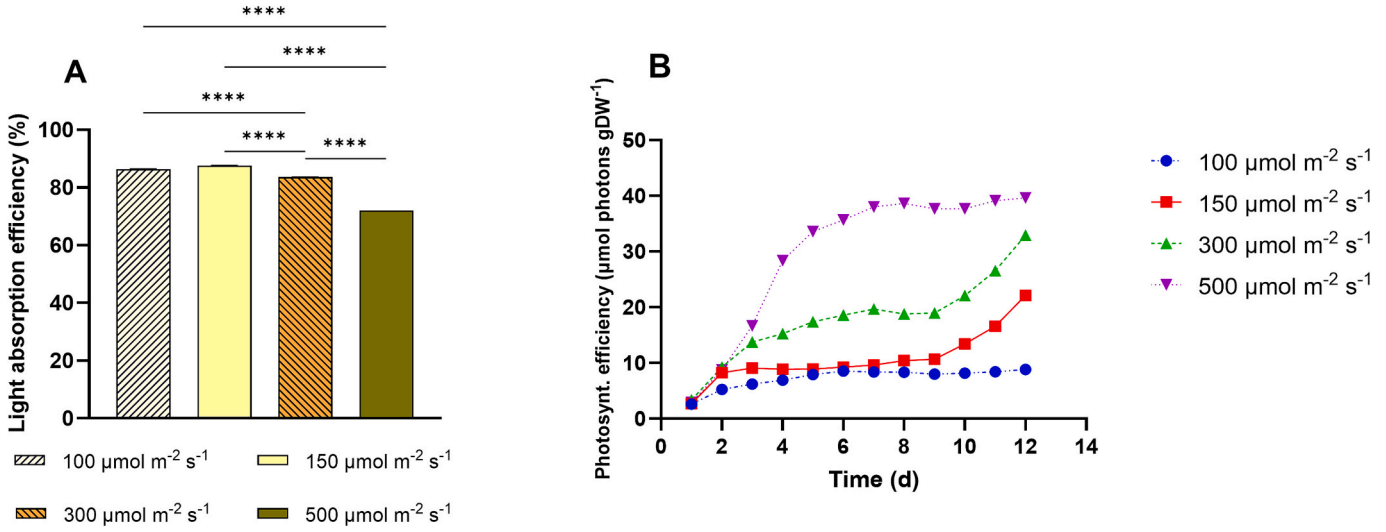

Fig. 3. Light transmission data under four light intensities. A) Light absorption efficiency, expressed as ratio between the light actual absorbed and the light perceived by the cell culture. B) Photosynthetic efficiency, expressed as µmol photons per gram of biomass produced.

by the cyanobacterial culture, for all the nominal light intensities tested here. Therefore, at 100 and 150 µmol photons m^{-2} s^{-1} cells used up to the 87 %, then, this percentage dropped to 83 % and 72 % at 300 and 500 µmol photons m^{-2} s^{-1}, respectively (Fig. 3A).

Furthermore, for each light condition photosynthetic efficiency (Fig. 3B, C) was calculated as absorbed photons per gram of biomass produced through photosynthesis (Schuurmans et al., 2015) (Supplementary Table S1, Eq. 34). For any kind of PBR, the photosynthetic efficiency can be evaluated considering the whole PBR system, from the incident light (I_{in}) to the vessel, passing through the liquid, where the cyanobacteria move around (I_{out}). Particularly, we measured the photosynthetic efficiency experimentally and estimated through model simulations that account for light absorption by both all the domains considered in the model and cyanobacteria, and the light scattering due to the gas bubbles (Supplementary Fig. S1C). The efficiency was then derived by relating the growth rate and dry weight measurements to the absorbed light. Therefore, the photosynthetic efficiency indicates the µmoles of photons utilised for producing 1 g of biomass. Thus, especially for batch cultivations, the lower the photosynthetic efficiency the higher the light utilisation efficiency (Fig. 3B). Indeed, the photosynthetic efficiency of the system was highest in each light condition at the end of the test, when the cell population was the densest (Fig. 3B). The greatest change was recorded for the highest photon fluxes, where the photosynthetic efficiency increased quickly by 13 folds of the initial value (2.95 µmol photon g DW^{-1}), while at the lowest light intensity it rose only by 3 folds (Fig. 3B). An increase in the photosynthetic efficiency means that more photons need to be provided to produce the same amount of biomass as cell density increases (Fig. 2C). From this evaluation it is evident how much the cell density affects this important parameter in bioprocess design; indeed, the photosynthetic efficiency is equal for all the light conditions tested after the first day of investigation, where the biomass was produced linearly to the amount of light supplied.

To validate the model, the light transmission data, as light incident (I_{in}) and light transmitted (I_{out}), were collected experimentally in both abiotic and biotic conditions and used to build the model. The model validation is reported in Supplementary Fig. S5.

3.3. 2-Phenylethanol production by 2PE_aroK mutant strain

The ability to produce 2-PE resulted to be strongly affected by the light intensity. Fig. 4A shows the 2-PE production kinetics under four increasing light intensities. As expected, in dark condition, 2-PE was not produced at all (Table 2), thereby, all the data about the dark condition were eliminated from any representation hereinafter.

The highest and lowest 2-PE concentrations were achieved at 150 and 500 µmol photons m^{-2} s^{-1}, respectively (Fig. 4A, B). Particularly, at 150 µmol photons m^{-2} s^{-1}, we recorded a concentration of 282 ± 21.1 mg L^{-1} 2-PE. This result aligns well with previous data for the same mutant strain, which reported 285 mg L^{-1} 2-PE in shaking flasks (Usai

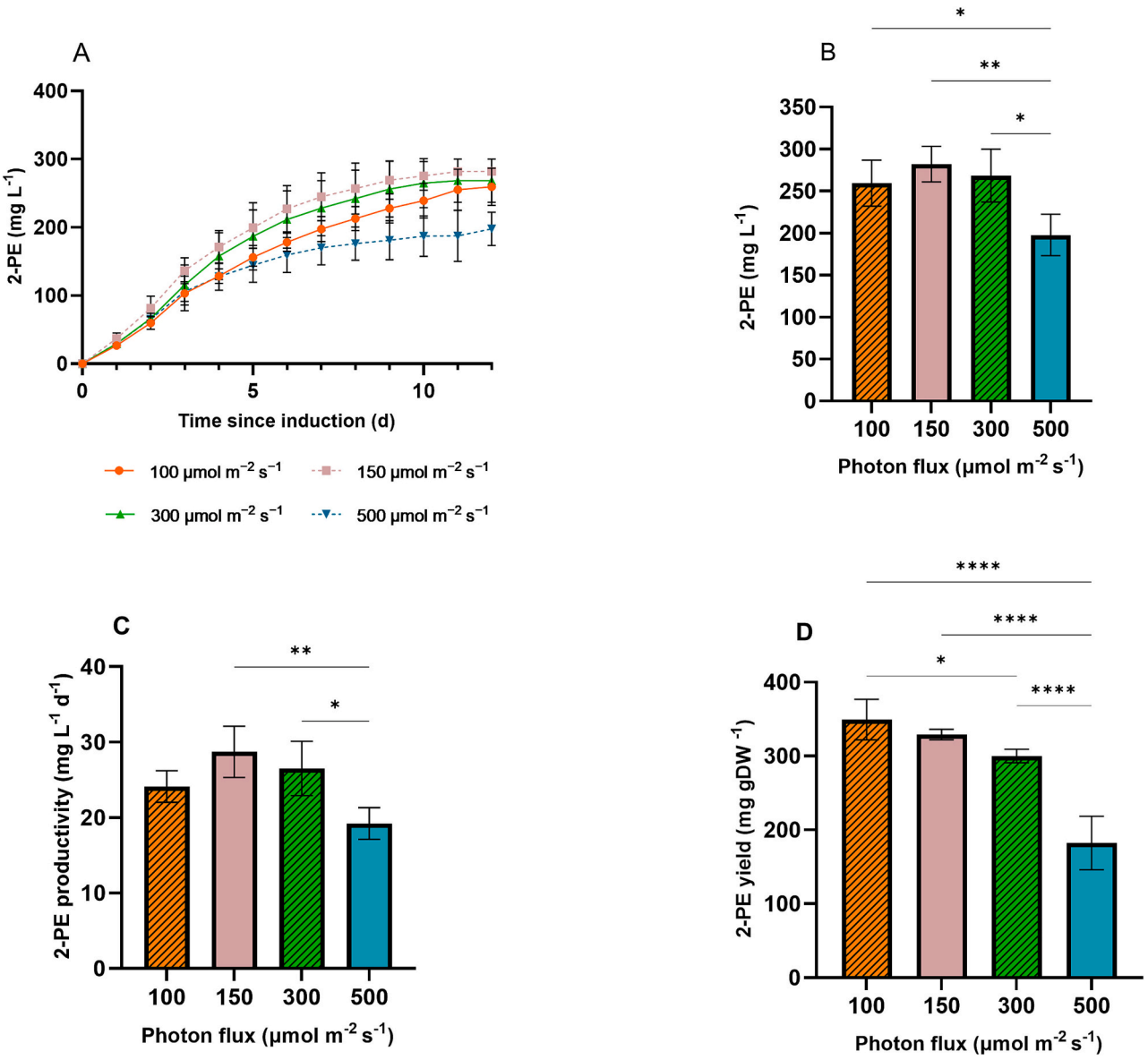

Fig. 4. 2-PE-related data of the 2PE_*aroK* mutant strain exposed to four light conditions in batch mode. A) 2-PE kinetics production; B) 2-PE final concentration; C) 2-PE volumetric productivity; D) 2-PE production normalised by the biomass necessary for producing 2-PE, expressed as mg of 2-PE per gDW. All the tests were carried out as four biological replicates. Error bars represent standard deviation. The statistics was performed as one-way ANOVA ($\alpha \leq 0.05$). Asterisks refer statistical significance. *, *p*-value ≤ 0.05; **, *p*-value ≤ 0.002; ***, *p*-value ≤ 0.0002; ****, *p*-value ≤ 0.0001.

et al., 2022). However, in the current study, we reached 282 mg L^{-1} in just ten days of production time, significantly increasing volumetric productivity to 28.7 ± 3.4 mg L^{-1} d^{-1} (Fig. 4C). This results as the highest 2-PE volumetric productivity reported under photoautotrophic conditions to date. Furthermore, at the highest photon flux, i.e. 500 µmol m^{-2} s^{-1}, the 2-PE production was calculated as 198 ± 24.6 mg L^{-1}, resulting in a 30 % decrease if compared to the highest 2-PE accumulation (Fig. 4B). Consequently, the 2-PE yield resulted to be lower if compared to the lowest photon fluxes, where the yield ranged 339–349 mg of 2-PE per gram of dry cell biomass (mg g DW^{-1}, Fig. 4D, Table 2). Overall, the most intense light condition (500 µmol photons m^{-2} s^{-1}) seems not to guarantee the best results in terms of target compound. Indeed, photosynthesis and 2-PE production likely uncoupled at light intensities exceeding 300 µmol photons m^{-2} s^{-1}, where increasing the photosynthesis-linked carbon flux had no positive effect on target compound synthesis. Thus, increasing light intensity to boost photosynthesis led to biomass accumulation, which strongly competed with 2-PE production (Fig. 4B, D).

3.4. *Effect of photon flux on CO_2 and L-phenylalanine uptake*

1 % CO_2 was supplied in a mixture with N_2 with a gas flow rate of 150 mL min^{-1}. To start the 2-PE production phase we added 1 mM IPTG and 0.3 g L^{-1} L-Phe into the PBR, when the bacterial reached $OD_{730} = 1$ and the data collection stopped when the 2-PE productivity became negligible (after about 10–12 days). Therefore, the present bioprocess was fed with both CO_2 and L-Phe, and their uptake appeared to be strongly influenced by the photon flux. In the dark production condition, neither CO_2 nor L-Phe resulted to be consumed (data not shown), indicating that light is the essential driving force of the present biomanufacturing process. Furthermore, the L-Phe consumption was found to be severely altered; the higher the light intensity, the lower the L-Phe uptake (Fig. 5A). At the highest light intensities, i.e. 300 and 500 µmol m^{-2} s^{-1}, cyanobacteria consumed only 33 % and 46 % of the available L-Phe, respectively. Conversely, nearly all the available L-Phe was taken up at 150 (78 %) and 100 (79 %) µmol photons m^{-2} s^{-1}. The CO_2 consumption was also affected, and the highest amount was recorded at

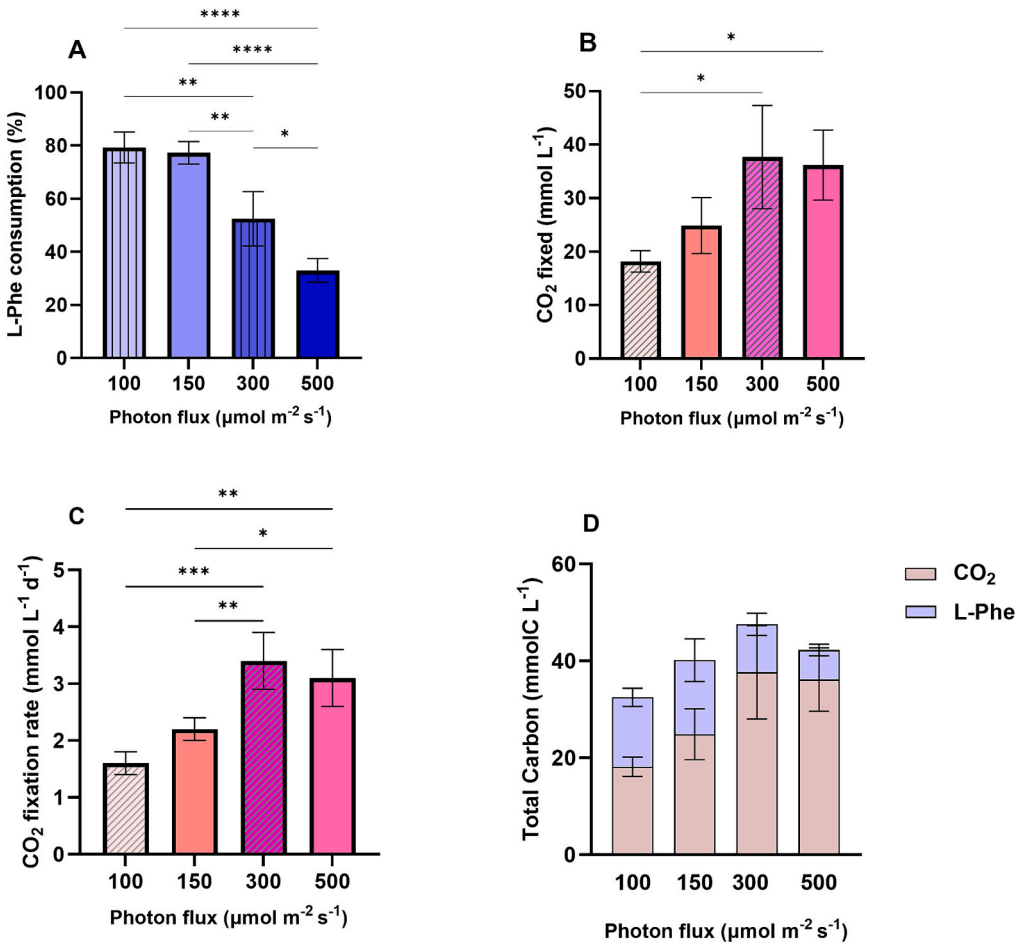

Fig. 5. Carbon consumption results of the 2PE_aroK mutant strain exposed to four light conditions in batch mode. A) Percentage of L-Phe consumed of the available one; B) carbon fixed through photosynthesis, expressed as mmol of carbon atoms consumed from the supplied CO_2; C) carbon fixation rate, expressed as mmol C L^{-1} d^{-1}; D) total amount of carbon consumed from CO_2 (pink bars) and L-Phe (violet bars). All the tests were carried out as four biological replicates. Error bars represent standard deviation. The statistics was performed as one-way ANOVA ($\alpha \leq 0.05$). Asterisks express statistical significance. *, *p*-value ≤ 0.05; **, *p*-value ≤ 0.002; ***, *p*-value ≤ 0.0002; ****, *p*-value ≤ 0.0001. (For interpretation of the references to color in this figure legend, the reader is referred to the web version of this article.)

the most intense light conditions (Fig. 5B), resulting in a CO_2 fixation rate of 3.1 mmol C L^{-1} d^{-1} during the production phase (Fig. 5C). On the other hand, at the lowest light intensity, the fixation rate resulted to be reduced by almost a half (1.6 mmol C L^{-1} d^{-1}, Fig. 5C). Fig. 5D reports the sum of the carbon atoms consumed from both CO_2 and L-Phe and it is expressed as mmol C L^{-1}. To what extent CO_2 and L-Phe were exploited into the present bioprocess will be discussed in the following section.

The total carbohydrate content was determined as glycogen content, which serves as the primary storage compound for CO_2 fixed through photosynthesis in cyanobacteria (De Porcellinis et al., 2017), functioning as a crucial natural carbon sink. Our observations reveal that under low light conditions, glycogen accumulated steadily over time, constituting approximately 10 % of dry biomass. Conversely, in conditions of higher light intensity, glycogen content is higher and exhibits periodic fluctuations, although not statistically significant, reaching at the best up to 15 % of the biomass (Supplementary Fig. S6). This is coherent with an increased photosynthetic activity.

3.5. Carbon balance response to varying photon flux

All the carbon atoms coming from both the uptaken CO_2 and L-Phe were considered together to better understand how carbon atoms were differently distributed between biomass and 2-PE (Fig. 6A). Table 3 shows the detailed data on carbon analysis. At the highest light intensity (500 µmol photons m^{-2} s^{-1}), a larger percentage of carbon atoms (approximately 72 %) was directed towards biomass production. In contrast, under the other three light conditions, the percentage of carbon allocated to biomass ranged from 50 % to 54 % (Fig. 6A, green bars). Consequently, the percentage of carbon atoms as part of 2-PE ranged from 30 to 50 % (Fig. 6A, magenta bars). Beyond predictable relationship observed between the CO_2 uptake and high light condition, the most interesting results were about the L-Phe utilisation. As already mentioned, the L-Phe uptake lowered as the photon flux increased (Fig. 5A). Therefore, by assuming that the consumed L-Phe was fully employed to produce 2-PE, we calculated the L-Phe contribution for 2-PE synthesis. Theoretically, the yield between 2-PE (C8) and L-Phe (C9) is 89 %, thus, a dramatic difference between low and high light intensities emerged (Fig. 6B): under the two low light conditions, the consumed L-Phe might generate up to 78 % of the synthesised 2-PE; under the highest photon fluxes only the 43 % of 2-PE could be produced from L-Phe, and the residual 2-PE should has been synthesised from CO_2. Although higher light intensities result in a lower overall production of 2-PE, a greater proportion of the 2-PE that is produced comes directly from the photosynthesis, favouring CO_2 incorporation. Therefore, summing up all the results 150 and 300 µmol photons m^{-2} s^{-1} seemed to be the most successful production conditions. Finally, to better understand the nature of this bioprocess and its biocatalyst (i.e. 2PE_*aroK* mutant) we chose a light condition among the best ones and assayed the production of the 2-PE in semi-continuous (turbidostat) cultivation mode, as discussed later on.

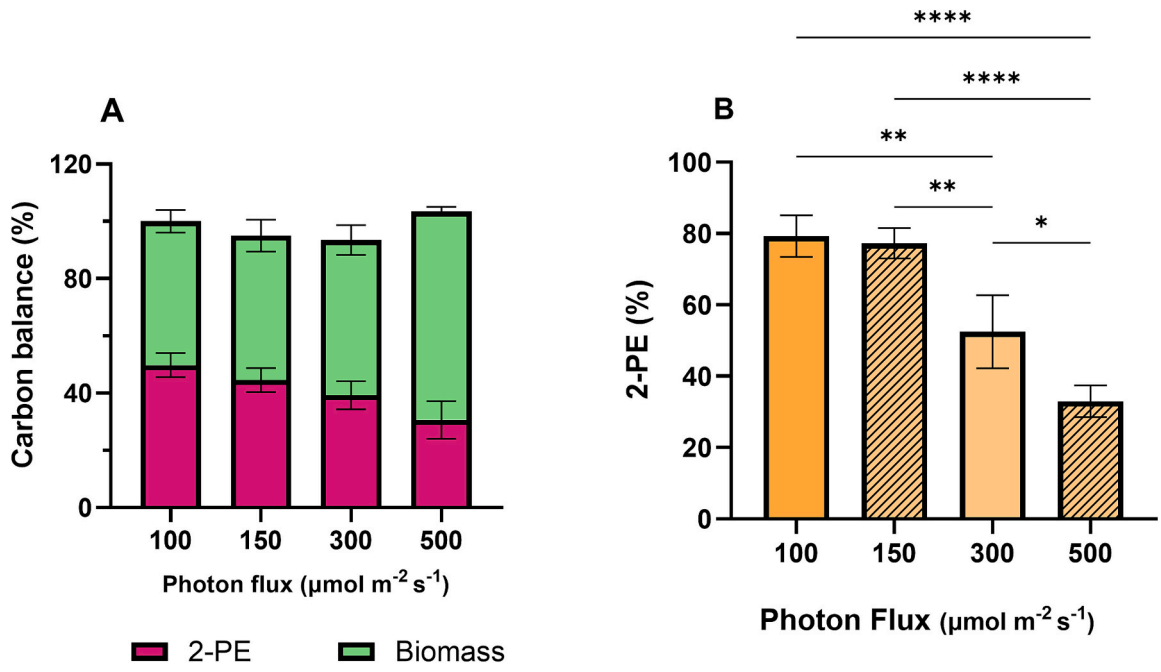

Fig. 6. Carbon distribution analysis of the 2PE_aroK mutant strain exposed to four light conditions in batch mode. A) Carbon balance indicates the percentage of the total consumed carbon atoms partitioning between 2-PE (magenta bars) and biomass (pink bars); B) percentage of 2-PE producible from the L-Phe effectively consumed in every light conditions. The experiments were conducted by the means of four biological replicates. Error bars refer to standard deviation. (For interpretation of the references to color in this figure legend, the reader is referred to the web version of this article.)

Table 3
Summary of the carbon-related data obtained from the liquid batch cultures exposed to four different light conditions.

Photon flux (µmol photons m^{-2} s^{-1})	CO_2 fixed (mmol C L^{-1})		CO_2 fixation rate (mmol C L^{-1} d^{-1})		L-Phe consumed (mmol C L^{-1})		C balance (%)				2-PE/L-Phe (%)		Final glycogen content (%DW)	
							Biomass		2-PE					
	Average	SD	Average	SD	Average	SD	Average	SD	Average	SD	Average	SD	Average	SD
100	18.2	2	1.6	0.2	14.3	1.9	50.3	3.9	49.7	4.2	78.6	3.1	11.2	2.7
150	24.9	5.2	2.2	0.2	15.3	4.4	50.5	5.6	44.5	4.2	78.1	12.8	10.4	0.9
300	37.7	9.6	3.4	0.5	9.9	2.3	54.2	5.2	39.3	4.9	42.6	11.5	12.2	0.9
500	36.2	6.5	3.1	0.5	6.1	1.2	72.9	1.6	30.6	6.5	42.5	8.6	13.3	1.1

3.6. Photosynthetic pigments content in 2PE_aroK mutant strain

Phycocyanin (phy), chlorophyll *a* (chla) and total carotenoids (car) were quantified. Chla is the main pigment involved in photosynthesis, particularly in light harvesting as well as in converting energy of absorbed photons to chemical energy. Chla is universally distributed in all the oxygenic photosynthetic organisms and in small amount in green sulfur bacteria and anaerobic phototrophs. Other chlorophylls (e.g. b, c, d, f) are diffused differently among cyanobacteria, microalgae, macroalgae and higher plants (Björn et al., 2009). Here, the chla content resulted constant over the time and among the light intensities (Fig. 7A), with some slight differences but not statistically significant. Indeed, the chla content in cyanobacteria tends to be constant unless the microorganisms are subjected to very stressful conditions (e.g. light, temperature, nitrogen and phosphorous depletion (da Silva Ferreira and Sant'Anna, 2016; Rahman et al., 2023)). That does not seem the case of our investigation. Similarly, the content in carotenoids appeared to be higher according with the highest light intensity exposure (Fig. 7B). Carotenoids are well-known to be associated with stress conditions, particularly those related to light, as part of the cells initial response (Masojídek et al., 2013; Lopes et al., 2020). Consistently, in our investigation, the largest carotenoids content was recorded for the highest light intensity following the gene expression induction. This data could be due to 24 h exposure at 500 µmol photons m^{-2} s^{-1} before the production phase induction. However, even if the light was gradually increased during the 1st stage of this bioprocess (i.e. cellular growth), probably this exposure could cause that carotenoids rise, which relaxed in the following days.

Currently, phycocyanin is one of the most explored natural pigments. It is water-soluble and blue-coloured, and contributes significantly to the natural shade of cyanobacteria, also known as blue-green algae. Here, we quantified phy in our mutant strain of *S. elongatus* PCC 7942, 2PE_*aroK*, in non-targeted condition for pigments production. Thus, we detected the highest amount at the lowest light intensities (Fig. 7C). Over the time, the amount of phy evolved, especially at both the highest light intensities, where the phy content decreased from 3 to 1.3%DW at the end of the experiment. Also, at the lowest photon fluxes the quantified phy decreased within ten days by 24 and 45 % of the initial amount at 100 and 150 µmol photons m^{-2} s^{-1}, respectively (Fig. 7C).

3.7. 2PE_aroK mutant strain characterisation in turbidostat mode

One of the most promising light conditions tested in batch mode was selected for further analysis in turbidostat cultivation mode. The recombinant strain was subjected to semi-continuous cultivation as follow: 1 % CO_2 (150 mL min^{-1} in N_2), 30 °C and the periodical dilution was performed to keep the OD_{730} constant to 1 (± 3 %), by adding fresh medium supplemented with 1 mM IPTG and 0.3 g L^{-1} L-Phe. The photon

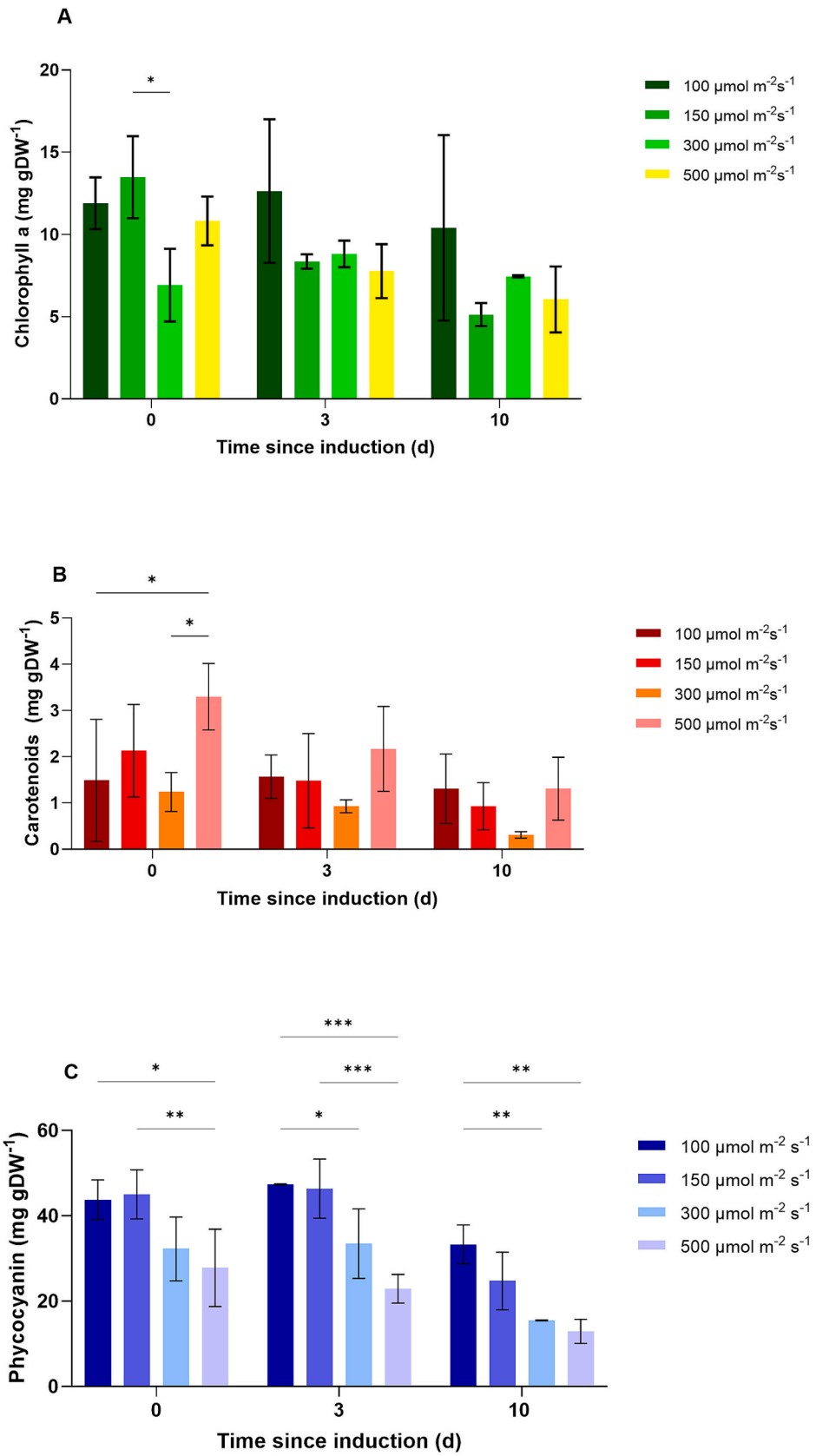

Fig. 7. Photosynthetic pigment profile of the 2PE_aroK mutant strain exposed to four light conditions in batch mode. A) Chlorophyll a; B) total carotenoids; C) phycocyanin. All the tests were carried out as four biological replicates and the results are expressed as mg of pigment per g of dry cell weight (mg g DW^{-1}). Error bars represent standard deviation. The statistics was performed as two-way ANOVA ($\alpha \leq 0.05$). Asterisks express statistical significance. *, p-value ≤ 0.05; **, p-value ≤ 0.002; ***, p-value ≤ 0.0002; ****, p-value ≤ 0.0001.

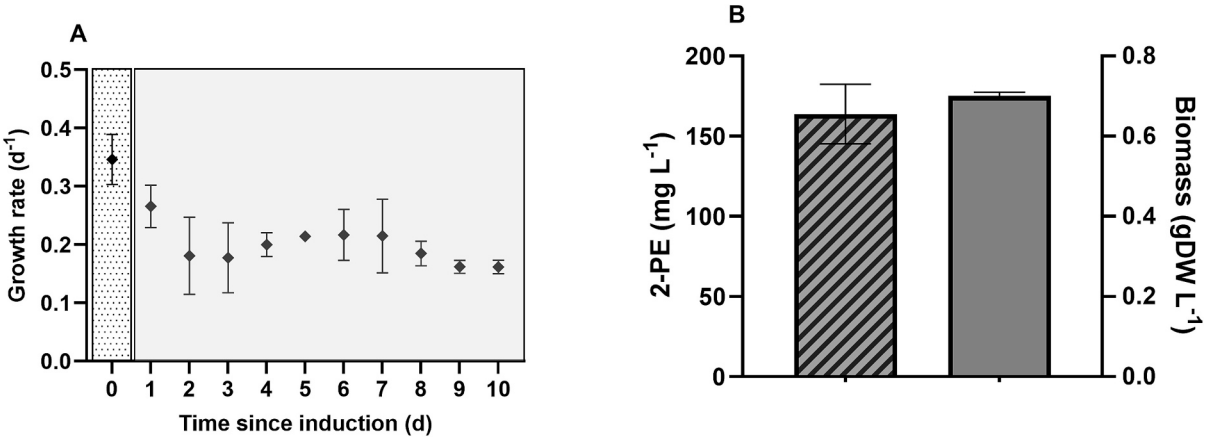

Fig. 8. 2PE_*aroK* mutant strain under turbidostat cultivation mode at 150 µmol photons m^{-2} s^{-1}. A) Growth rates calculated over the time before (dotted box) and after the gene expression induction and metabolite doping (grey full box). B) Biomass accumulation, as the sum of the biomass calculated from each turbidostat cycle, and 2-PE production in turbidostat mode. All the experiments were performed by the means of biological triplicates. Error bars represent standard deviation.

flux was set at 150 µmol m^{-2} s^{-1}. This cultivation mode allowed to get knowledge about the combinatorial effect of light exposure and 2-PE production phase induction. Fig. 8A reports the growth rate over the time before and after the gene expression induction within ten days of production phase at 150 µmol photons m^{-2} s^{-1}. Noteworthy, the growth rate stabilised after two days, and on average it halved with respect of the growth rate before inducing the production stage (Fig. 8A, dotted box). This finding suggests that inducing gene expression and metabolite doping actually might provoke a slowdown of the cell fitness (detailed representation is reported in Supplementary Fig. S7). The final biomass production in this cultivation condition was found to be 0.7 g DW L^{-1} (Fig. 8B), which was slightly improved if compared to the biomass accumulation in batch mode at the same light condition (Fig. 2B). On the other hand, the 2-PE synthesis was severely reduced to 164 mg L^{-1} at the end of the test (Fig. 8B), decreasing by 42 % in 2-PE production abilities of the recombinant strain. The present operative modes comparison suggested that the batch cultivation outdid the turbidostat one, considering 2-PE biomanufacturing.

4. Discussion

Although many strains of cyanobacteria, both recombinant or wild-type, have been studied for the biomanufacturing of high-value compounds, significant technical and scientific efforts are still required to develop effective scalable bioprocesses. Notoriously, the physiology of cyanobacteria and eukaryotic microalgae strongly changes when grown in photobioreactors (PBRs) if compared to the standard and comfortable laboratory equipment, e.g. Erlenmeyer flasks. Indeed, we can better tune several parameters in PBR, such as light exposure, light diffusion, CO_2 supply, mixing, temperature and pH. Consequently, biological factors (e.g. growth rate, biomass production, target compound productivity, carbon uptake, etc.) could evolve differently during a scale-up process. Thus, a systematic analysis becomes obligatory to find the engineering rules suitable for a specific cyanobacteria-based bioproduction. Accordingly, often the light resulted to be the limiting factor mainly impacting on photoautotrophic bioprocesses. Here, we studied the production ability of a metabolically engineered strain of *Synechococcus elongatus* PCC 7942 to heterologously produce 2-PE in FMT150 photobioreactor (PBR), when subjected to different photon fluxes. The FMT150 PBR (Nedbal et al., 2008) is a flat panel reactor system, in which the surface area per culture volume is maximised, so, it is the best tool to study the effect of light irradiance to the cell physiology. The abovementioned mutant strain, already published elsewhere, is capable of synthesising 2-PE by overexpressing five genes (Usai et al., 2022). Table 1 reports the genetic features of this recombinant strain, also known as 2PE_*aroK*, and the relative protein products involved in this heterologous 2-PE pathway (Fig. 1). The 2PE_*aroK* has been previously reported to produce up to 285 mg L^{-1} 2-PE in three weeks when doped with 0.3 g L^{-1} L-Phe in shaking flask (Usai et al., 2022) and, recently, 180 mg L^{-1} 2-PE in ten days when cultivated in a blend of dairy wastewater (Usai et al., 2024), further supporting its industrial relevance.

4.1. Growth kinetics under varying light intensity

Here, the 2PE_*aroK* mutant strain was subjected to four light intensities (100, 150, 300 and 500 µmol photons m^{-2} s^{-1}) and dark condition in a liquid batch operational mode, constituted of two separate stages: i) growth and light acclimation stage (until the culture reaches $OD_{730} = 1$); ii) 2-PE production stage (triggered by the addition of 1 mM IPTG and 0.3 g L^{-1} L-Phe as gene expression inducer and metabolite doper, respectively). As anticipated, biomass accumulation increased with higher light intensity (Fig. 2A and B), but this relationship was non-linear (Fig. 2C). Indeed, the growth rate at the highest photon flux grew only by 19 % if compared to that at the lowest light condition (Fig. 2C, Table 2). These data suggested a mild self-shading effect (Agustí, 1991), where the high cell density (reaching around 1 g DW L^{-1}) might reduce the light penetration into the vessel by limiting further biomass production.

4.2. Light distribution in flat-panel PBR under 2-PE production condition

Thus, to ultimately study the light distribution into the vessel of the PBR when cultivating the mutant strain, we used a 3D model already developed by us (Vasile et al., 2021; Cordara et al., 2018). The COMSOL 6® model's operational conditions were designed to closely match those tested experimentally in the flat panel PBR. These included varying light intensities and different cultivation modes (e.g. batch and semi-continuous) to simulate experimental setups accurately. The model successfully replicated key experimental observations, such as the cyanobacterial growth rate, the transmission and absorption of light within the domains of the reactor, and the bioprocess efficiencies (Fig. 3). Thus, mimicking realistic experimental conditions in silico should be a standard approach to accelerate bioprocess design for specific applications. Here, we evaluated how the light distribution is affected by the cell concentration and growth rates. Indeed, the biosystem (comprising the cell culture and the PBR) was able to utilise 72 % of the incident light at the highest light intensity, compared to 87 % at the lowest photon flux (Fig. 3A), indicating greater light absorption efficiency at lower photon flux. An important parameter to consider is photosynthetic efficiency,

expressed as μmoles of photons employed to produce 1 g of biomass across four light intensities (Fig. 3B). Our simulation showed that higher light intensities led to increased cell density but also raised the effort required to produce additional biomass (Fig. 3), and, so, increasing costs associated with light supply. Deepening these aspects prior to engage bioprocess development, allows for tailored tests specific to each PBR geometry, backed by solid data (Vasile et al., 2021; Zhang et al., 2024).

4.3. 2-PE production depends on the light intensity

In agreement with the data from the light absorption analysis, we measured that at the three lower light conditions (100, 150 and 300 μmol photons m^{-2} s^{-1}) the 2-PE concentration was the highest, i.e. 260–282 mg L^{-1} (Fig. 4A, B). Therefore, a reduced biomass production did not correspond to a diminished 2-PE production (Fig. 4B, C). Notably, at 150 μmol photons m^{-2} s^{-1} we achieved the highest 2-PE productivity reported so far via photoautotrophy and metabolite doping (Fig. 4C). A 2-PE productivity of 28.7 ± 3.4 mg L^{-1} d^{-1} represents a significant achievement in our study, markedly reducing the production time of this commercially valuable molecule compared to previously reported values (Usai et al., 2022). On the other hand, at the highest light condition of 500 μmol photons m^{-2} s^{-1}, the 2-PE concentration was severely compromised, dropping by 30 % compared to the peak production, resulting in only 198 mg L^{-1} (Fig. 4B). This observation is even more pronounced when considering the 2-PE yield normalised per g of dry biomass (Fig. 4D). At the lowest light intensities, less biomass is needed to achieve the highest 2-PE production. Consequently, at 100 and 150 μmol photons m^{-2} s^{-1}, the yields were 350 and 329 mg g DW^{-1}, respectively, which represent the highest 2-PE yields reported under photoautotrophic conditions to date (see Table 2 for more details). Therefore, this study suggests how increasing the carbon flow through photosynthesis does not necessarily lead to the best performance, as targeted production, while the excess of carbon atoms is preferentially regulated via biomass accumulation. These findings are consistent with some biochemical investigations concerning the competition for metabolic precursors between biomass synthesis and target production, showing that they could be mutually exclusive (Pérez et al., 2019; Du et al., 2018a; Du et al., 2017). Furthermore, Erdrich et al. (2014) proposed an in silico modelling study on the metabolism of the model cyanobacterium *Synechocystis* sp. PCC6803. They suggested that to prevent an imbalance between growth and desired production, the target product should serve as a sink for reducing equivalents within the cell. Moreover, they added that a moderate increase of ATP turnover or energy dissipation is a promising approach to correct the stoichiometry necessary to balance biomass and target product synthesis. Thus, here, we theoretically exploited a functional carbon sink for photoautotrophic production regime. Indeed, the 2PE_*aroK* mutant strain produces 2-PE by alcohol dehydrogenase A using NADPH, as final step of the heterologous pathway (Fig. 1). Additionally, the *aroK* gene overexpression by the 2PE_*aroK* mutant strain, led to overproduce the shikimate kinase, a protein involved in the shikimate pathway and consuming ATP as co-substrate (Fig. 1). The effectiveness of the shikimate kinase overexpression was already reported as essential to really improve 2-PE production in 2PE_*aroK* mutant (Usai et al., 2022), especially when compared to the previously described cyanobacterial mutants for 2-PE biomanufacturing (Ni et al., 2018). To get a comprehensive view of our bioprocess, we considered that the carbohydrate synthesis pathway is the most competitive, because cyanobacteria store glycogen as the main energy reserve. Accordingly, we observed an increased glycogen accumulation into the mutant biomass exposed to the highest photon fluxes (Supplementary Fig. S6). In the literature, many studies have attempted to impair or disrupt glycogen metabolism, often leading to severely reduced cell fitness or an overflow of intermediate metabolites (Luan et al., 2019; Cano et al., 2018). However, due to the high content in carbohydrates, as glycogen (or starch in eukaryotic microalgae), and proteins, the exhausted cyanobacterial/microalgal biomass might be used for further valorisation as feedstock or additive for yeasts or bacterial fermentations (Comer et al., 2020; Hays and Ducat, 2018).

4.4. Carbon uptake and allocation are influenced by light intensity

Thoroughly studying the delicate relationship between light and carbon inputs is crucial for balancing resources in a photosynthetic microbial factory and ensuring process sustainability. Indeed, our analysis of carbon fate within the cell provides valuable insights into this topic (Fig. 5, Fig. 6, Table 3). The carbon atoms taking part of the 2-PE or biomass could come from both CO_2 and L-Phe (supplemented as metabolite doper). As expected, at the highest light intensities assessed (i.e. 300 and 500 μmol photons m^{-2} s^{-1}) the amount of fixed carbon atoms and CO_2 fixation rate were the highest (Fig. 5B, C). However, we noticed that the higher the light intensity, the lower the L-Phe uptake (Fig. 5A). L-Phe uptake in wild-type *S. elongatus* PCC 7942 and other cyanobacteria strains has been previously reported (Usai et al., 2022; Kukil et al., 2023), and, also, uptaking L-Phe is energy-demand (Labarre et al., 1987). We already speculated (Usai et al., 2022) that the combination of some of the overexpressed proteins in 2PE_*aroK* mutant (*kivD* and *adhA* protein products) might reproduce a sort of Ehrlich pathway, usually exploited in yeast for the production of 2-PE starting from L-Phe (Gu et al., 2020; Dai et al., 2021). Nevertheless, this speculation provides no extra explanation about the massive effect of shikimate kinase (*aroK* gene) overexpression (located upstream to this putative Ehrlich pathway) on 2-PE production. Currently, to the best of our knowledge, there are no further indications regarding the use of L-Phe once inside the cells. Therefore, this topic warrants additional investigation to be effectively applied in aromatic bioproduction, which, to date, is a flourish and valuable topic for biotechnology (Dickey et al., 2024; Masuo, 2024).

Carbon balance analysis was conducted in this study and highlights how the carbon atoms partition differently between biomass and target product (i.e. 2-PE). Firstly, carbon atoms from CO_2 contributed more than L-Phe in all the light conditions tested (Fig. 5D), particularly, by 56 % and 86 % of the total carbon atoms used at the lowest and highest light intensities, respectively. More in detail, at the highest light intensity up to 72 % of carbon atoms were employed to build biomass despite of 2-PE (Fig. 6A). At the two lowest photon fluxes, 50 % and 45 % of carbon atoms were directed to synthesise 2-PE (Fig. 6A). Increasing the carbon partitioning towards the target compound so that it is ≥50 % is one of the desirable goal in creating a bioprocess, necessary for qualifying such a strain as a photosynthetic microbial factory (Ducat et al., 2012; Gao et al., 2012; Savakis et al., 2013). No other by-product was considered for the present carbon analysis. Indeed, cyanobacterial photoautotrophic metabolism releases relatively few metabolic intermediates into the extracellular space (Pérez et al., 2019). Therefore, the present estimated carbon balance should be quite accurate. To better understand the extent to which consumed L-Phe contributes to 2-PE production, we based our analysis on the theoretical yield of 2-PE (C_8) production from L-Phe (C_9), which is 89 %. Significantly, at the highest light intensities of 300 and 500 μmol photons m^{-2} s^{-1}, only 42 % of 2-PE could be synthesised from L-Phe under those conditions, while at the lowest photon fluxes this percentage increased to 78 % (Fig. 6B). This evaluation assumes that the total amount of metabolised L-Phe was used exclusively for 2-PE production, without competition from biomass synthesis or other collateral pathways. However, these findings indicate that, despite the lower final 2-PE concentration at the highest light intensity, a larger proportion (at least 60 %) is likely produced from CO_2 rather than L-Phe. Thus, this phenomenon inspires different observations. Traditionally, bioprocess engineering approaches focus on target compounds, with all the steps designed to maximise productivity, by adopting ideal conditions and rich synthetic media. On the other hand, the opportunity to exploit flue gas streams with high CO_2 concentration (3–85 vol.%) (Zieliński et al., 2023) makes the CO_2 fixation abilities of cyanobacteria and microalgae even more appealing (Higashide et al., 2011; Yen et al.,

2015). Therefore, designing tailored bioprocesses for CO_2 capture from flue gas would be both economically and environmentally beneficial, even if, as demonstrated in our study, target molecule productivity may be partially reduced.

4.5. Valorisation of residual biomass: phycocyanin recovery

While the aim of this work is the characterisation of the 2PE_*aroK* recombinant strain abilities when exposed to different light conditions, it is still important to stress the opportunities of an exhausted cyanobacterial biomass and the target compound is not biomass-related but extruded into the culture broth. The cyanobacterial biomass is rich in photosynthetic pigments, and among them, phycocyanin (phy) is one of the most studied and it has a huge global market size, which will reach $6.3 billion by 2028 (Fernandes et al., 2023). Over the year, the phycocyanin has been investigated for anti-oxidation effect, anti-cancer and anti-inflammatory activities, photo-induced cytotoxicity and the capacity of stimulate the immune system (Pleonsil et al., 2013; Zhu et al., 2016). Besides the clinical potential applications, phycocyanin is largely required for food and beverages, nutraceutics and cosmetics (Fernandes et al., 2023). Biologically, phycocyanin is a pigment-protein complex and a major component of cyanobacterial light-harvesting antenna, which optimises light energy gathering, where the chlorophyll cannot absorb. Accordingly, the quality and intensity of the light significantly influence the light-harvesting system of cyanobacteria, affecting mostly the accumulation of photosynthetic pigments (Hsieh-Lo et al., 2019; Szwarc and Zieliński, 2018). When the light is low enough, the production of phy is intensified to catch as much light as possible. Accordingly, we quantified a higher amount of phycocyanin in biomass grown at lowest light intensities (Fig. 7C). At the moment of the induction of gene expression, the phy amount counted for 44 and 45 mg g DW^{-1} at 100 and 150 μmol photons m^{-2} s^{-1}, respectively. Afterwards, the phy amount decreased by 24 % and 45 % at the end of the experiment (Fig. 7C, 10th day), probably indicating the beginning of the stationary phase, as shown from the growth kinetics in Fig. 2A. At the highest light conditions, phy was lowered and at the end of the tests the amount was reduced over by 50 % (Fig. 7C). Regarding the other main photosynthetic pigments, i.e. the chlorophyll *a* (chla) and carotenoids (car), no particular trends were detected (Fig. 7A, B). The evolution over the time of the cellular composition about the photosynthetic pigments can be adopted as a physiological parameter to detect potential stress conditions, such as light excess or nutrient depletion, affecting the culture fitness. However, the present study has been conducted in excess of nutrients and CO_2, in standard synthetic medium, in order to focus only on the light effect. Indeed, the data on the pigment composition did not indicate any light stress of the mutant biomass.

4.6. Batch and semi-continuous cultivations highlight metabolic constraints in 2-PE production

Following the batch tests, the optimal light condition (150 μmol photons m^{-2} s^{-1}) was compared to semi-continuous (particularly turbidostat) cultivation mode to further elucidate the relationship between carbon flux influenced by photosynthesis and 2-PE synthesis as interdependent processes in this bioprocess. Since the culture density inside the PBR is maintained at a constant level (±3 %), the effect of light intensity on cyanobacterial physiology can be better assessed over time. In this study, the turbidostat mode started ca. 24–48 h before the gene expression induction and metabolite doping, in order to acclimate the culture to both the light and the cultivation mode. As in the batch mode, the gene expression and metabolite doping were activated by adding 1 mM IPTG and 0.3 g L^{-1} L-Phe, respectively. The periodical dilutions to maintain the cell density constant were performed with standard medium supplemented with 1 mM IPTG and 0.3 g L^{-1} L-Phe, not to washout the two molecules. The effect of the gene expression conveyed as a decrease in the growth rate of the mutant culture (Fig. 8A). The growth rate stabilised from the 2nd day at an average value of 0.17 ± 0.02 d^{-1} (Fig. 8A, grey box), which is almost half of that one measured before inducing the gene expression (Fig. 8A, dotted box). While the biomass production was only slightly improved (Fig. 8B) compared to the batch cultivation (Fig. 2B, Table 2), the 2-PE production was significantly affected with a reduction by >40 % compared to the 2-PE concentration obtained in batch mode (Fig. 8B). Consequently, the volumetric productivities were also disturbed, counting for 16.4 mg L^{-1} d^{-1}, 1.75-fold lower than that recorded in the batch study. Thus, as previously postulated for high light conditions, increasing the metabolic rate at the photosynthesis level further uncoupled the carbon flux into the heterologous 2-PE biosynthetic pathway, dramatically affecting target production. For these reasons, no additional higher light intensities were considered; instead, the main objective was to identify the optimal and least energy-consuming process conditions for bioproducing 2-PE. Interestingly, selecting specific light spectra may help to enhance the bioprocess. For instance, red light is widely recognized for stimulating photosynthesis by inducing the synthesis of PSI and PSII, whereas blue light has been found to significantly inhibit the growth rate of cyanobacteria (Luimstra et al., 2018). our findings indicate that red light, by stimulating the photosynthetic apparatus, may reduce 2-PE yield, while blue light, by modulating metabolic flow, could be leveraged as a bioprocessing strategy to enhance final bioproduction.

Additionally, the system developed in this study demonstrates competitive potential compared to established benchmarks such as yeasts and *E. coli*. In recent years, significant scientific efforts have focused on optimizing 2-PE bioproduction. Heterotrophic systems like *Saccharomyces cerevisiae*, *Kluyveromyces marxianus*, and *E. coli* have achieved high titers of up to 4.5 and 2.5 g L^{-1}, respectively (Bernardino et al., 2024; Noda et al., 2024), but their reliance on costly organic substrates remains a limitation. In contrast, our platform utilizes CO_2 and low light as primary inputs, offering a more sustainable and potentially cost-effective alternative. Although many heterotrophic systems have demonstrated promising results at the laboratory scale, their performance and robustness at industrial scale remain to be fully validated. Most studies have been conducted under ideal and controlled conditions, highlighting the need for further scale-up efforts. While current titers and productivities are lower, the potential for reduced feedstock costs and improved scalability underpins its value in green biomanufacturing. An insightful study (Brewster et al., 2025) recently presents a valuable example of an integrated bioprocess for 2-PE production and extraction successfully implemented at industrial scale, providing important insights for yeast-based bioprocess development.

In a broader context, biotechnological production of 2-PE wants to offer a safer and more sustainable alternative to traditional chemical synthesis, due to milder process conditions, lower energy requirements, and the avoidance of toxic precursors. Among emerging strategies, photosynthesis-driven 2-PE production using engineered cyanobacteria or algae is particularly attractive. It builds on the benefits of microbial systems and further enhances sustainability by using CO_2 and light as primary inputs. These factors position photosynthetic platforms as a promising next-generation alternative for climate-friendly 2-PE production. To sum up, our work, in addition, provides useful information on design strategies and required steps for bioprocesses based on engineered photosynthetic microorganisms. From this investigation of light influence on 2-PE biomanufacturing, the convergence of all the experimental data with an in silico modelling allowed to build a precise and resource-optimised framework for producing high-value green chemicals exploiting the photosynthesis ability of cyanobacteria.

5. Conclusions

This study discusses the implications of bioproducing 2-PE (2-phenylethanol) using a metabolically engineered strain of *Synechococcus elongatus* PCC 7942 in photobioreactor under different light exposures. We found a non-linear relationship between photosynthesis, biomass

formation, and production of 2-PE, revealing that the highest light intensity did not correspond to maximum 2-PE production; instead, only biomass formation improved.

Our light distribution analysis indicated that increasing photon flux in batch cultivation compromised light utilisation efficiency, while carbon consumption analysis highlighted an intricate carbon balance. Notably, the best allocation of carbon atoms (45–50 %) to 2-PE occurred at the lowest light intensities (100–150 μmol photons m^{-2} s^{-1}), which, also, led to impressively improve 2-PE productivity (29 mg L^{-1} d^{-1}), the highest recorded in photoautotrophy to date.

Overall, the study demonstrates that a finely tuned bioprocess can effectively function as a microbial factory under optimal conditions of light supply. Importantly, dark production tests reaffirmed that light remains the essential driving force in this biomanufacturing process. Moreover, as the target product is secreted into the culture medium, the spent cell biomass can be valorised through pigment extraction and utilised as substrate or additive in other fermentation processes implemented in cascade.

Abbreviations

2-PE	2-phenylethanol
SKP	shikimate pathway
Phe	phenylalanine
aroK	gene encoding for shikimate kinase
IPTG	isopropyl β-D-1-thiogalactopyranoside
PBR	photobioreactor
Chl a	chlorophyll *a*
Car	carotenoids
Phy	phycocyanin

CRediT authorship contribution statement

Giulia Usai: Writing – review & editing, Writing – original draft, Methodology, Investigation, Formal analysis, Data curation, Conceptualization. **Nicolò Santi Vasile:** Writing – review & editing, Writing – original draft, Formal analysis. **Davide Scabello:** Writing – review & editing, Writing – original draft, Investigation. **Elena Mazzocchi:** Writing – review & editing, Writing – original draft, Investigation. **Debora Fino:** Writing – review & editing, Supervision, Project administration. **Candido Fabrizio Pirri:** Writing – review & editing, Project administration. **Barbara Menin:** Writing – review & editing, Writing – original draft, Supervision, Project administration. **Alessandro Cordara:** Writing – review & editing, Writing – original draft, Project administration, Methodology, Investigation, Conceptualization.

Declaration of competing interest

The authors declare that they have no known competing financial interests or personal relationships that could have appeared to influence the work reported in this paper.

Acknowledgements

The authors gratefully acknowledge the Fondazione Istituto Italiano di Tecnologia (CSFT@IIT Turin, Italy) for its financial support.

Appendix A. Supplementary data

Supplementary data to this article can be found online at https://doi.org/10.1016/j.biteb.2025.102216.

Data availability

Data will be made available on request.

References

Agustí, Susana, 1991. Light environment within dense algal populations: cell size influences on self-shading. J. Plankton Res. 13 (4), 863–871. https://doi.org/10.1093/plankt/13.4.863.

Berla, Bertram M., Saha, Rajib, Immethun, Cheryl M., Maranas, Costas D., Moon, Tae Seok, Pakrasi, Himadri B., 2013. Synthetic biology of cyanobacteria: unique challenges and opportunities. Front. Microbiol. 4 (August), 246. https://doi.org/10.3389/fmicb.2013.00246.

Bernardino, Ana R.S., Torres, Cristiana A.V., Crespo, João G., Reis, Maria A.M., 2024. Biotechnological 2-phenylethanol production: recent developments. Molecules. https://doi.org/10.3390/molecules29235761.

Björn, Lars Olof, Papageorgiou, George C., Blankenship, Robert E., Govindjee., 2009. A viewpoint: why chlorophyll A? Photosynth. Res. 99 (2), 85–98. https://doi.org/10.1007/s11120-008-9395-x.

Blanken, Ward, Cuaresma, Maria, Wijffels, René H., Janssen, Marcel, 2013. Cultivation of microalgae on artificial light comes at a cost. Algal Res. 2 (4), 333–340. https://doi.org/10.1016/j.algal.2013.09.004.

Branco Dos Santos, Branco, Du, Wei, Hellingwerf, Klaas J., 2014. Synechocystis: not just a plug-bug for CO_2, but a green *E. coli*. Front. Bioeng. Biotechnol. 2, 36. https://doi.org/10.3389/fbioe.2014.00036.

Brewster, Alessandro, Oudshoorn, Arjan, van Lotringen, Marion, Nelisse, Pieter, van den Berg, Emily, Luttik, Marijke, Daran, Jean-Marc, 2025. Inhibition control by continuous extractive fermentation enhances de novo 2-phenylethanol production by yeast. Biotechnol. Bioeng. 122 (2), 287–297. https://doi.org/10.1002/bit.28872.

Brey, Laura Furelos, Włodarczyk, Artur J., Bang Thøfner, Jens F., Burow, Meike, Crocoll, Christoph, Nielsen, Isabella, Zygadlo Nielsen, Agnieszka J., Jensen, Poul Erik, 2020. Metabolic engineering of *Synechocystis* sp. PCC 6803 for the production of aromatic amino acids and derived phenylpropanoids. Metab. Eng. 57, 129–139. https://doi.org/10.1016/j.ymben.2019.11.002.

Cano, Melissa, Holland, Steven C., Artier, Juliana, Burnap, Rob L., Ghirardi, Maria, Morgan, John A., Yu, Jianping, 2018. Glycogen synthesis and metabolite overflow contribute to energy balancing in cyanobacteria. Cell Rep. 23 (3), 667–672. https://doi.org/10.1016/j.celrep.2018.03.083.

Comer, Austin D., Abraham, Joshua P., Steiner, Alexander J., Korosh, Travis C., Markley, Andrew L., Pfleger, Brian F., 2020. Enhancing photosynthetic production of glycogen-rich biomass for use as a fermentation feedstock. Front. Energy Res. 8. https://doi.org/10.3389/fenrg.2020.00093.

Cordara, Alessandro, Re, Angela, Pagliano, Cristina, Van Alphen, Pascal, Pirone, Raffaele, Saracco, Guido, dos Santos, Filipe Branco, Hellingwerf, Klaas, Vasile, Nicolò, 2018. Analysis of the light intensity dependence of the growth of *Synechocystis* and of the light distribution in a photobioreactor energized by 635 Nm light. PeerJ 6 (July), e5256. https://doi.org/10.7717/peerj.5256.

Dai, Jun, Xia, Huili, Yang, Chunlei, Chen, Xiong, 2021. Sensing, uptake and catabolism of L-phenylalanine during 2-phenylethanol biosynthesis via the Ehrlich pathway in *Saccharomyces cerevisiae*. Front. Microbiol. 12 (February), 601963. https://doi.org/10.3389/fmicb.2021.601963.

De Porcellinis, Alice, Frigaard, Niels-Ulrik, Sakuragi, Yumiko, 2017. Determination of the glycogen content in cyanobacteria. J. Visual. Exp. 125, 56068. https://doi.org/10.3791/56068.

Dechatiwongse, Pongsathorn, Srisamai, Suna, Maitland, Geoffrey, Hellgardt, Klaus, 2014. Effects of light and temperature on the photoautotrophic growth and photoinhibition of nitrogen-fixing cyanobacterium *Cyanothece* sp. ATCC 51142. Algal Res. 5, 103–111. https://doi.org/10.1016/j.algal.2014.06.004.

Dickey, R.M., Gopal, M.R., Nain, P., Kunjapur, A.M., 2024. Recent developments in enzymatic and microbial biosynthesis of flavor and fragrance molecules. J. Biotechnol. 389, 43–60. https://doi.org/10.1016/j.jbiotec.2024.04.004.

Do, T., Van Do, Cam, Dinh, Cuc T., Dang, Mai T., Tran, Thuan Dang, Le, Truong Giang, 2022. A novel flat-panel photobioreactor for simultaneous production of lutein and carbon sequestration by *Chlorella sorokiniana* TH01. Bioresour. Technol. 345, 126552. https://doi.org/10.1016/j.biortech.2021.126552.

Drężek, Karolina, Antunovics, Zsuzsa, Grabiec, Agnieszka Karolina, 2024. Novel *Saccharomyces uvarum* × *Saccharomyces kudriavzevii* synthetic hybrid with enhanced 2-phenylethanol production. Microb. Cell Factories 23 (1), 1–10. https://doi.org/10.1186/s12934-024-02473-3.

Du, Wei, Angermayr, S. Andreas, Jongbloets, Joeri A., Molenaar, Douwe, Bachmann, Herwig, Hellingwerf, Klaas J., dos Santos, Filipe Branco, 2017. Nonhierarchical flux regulation exposes the fitness burden associated with lactate production in *Synechocystis* sp. PCC6803. ACS Synth. Biol. 6 (3), 395–401. https://doi.org/10.1021/acssynbio.6b00235.

Du, Wei, Caicedo Burbano, Patricia, Hellingwerf, Klaas J., dos Santos, Filipe Branco, 2018a. In: Zhang, Weiwen, Song, Xinyu (Eds.), Challenges in the Application of Synthetic Biology toward Synthesis of Commodity Products by Cyanobacteria via 'Direct Conversion' BT — Synthetic Biology of Cyanobacteria. Springer Singapore, Singapore. https://doi.org/10.1007/978-981-13-0854-3_1.

Du, Wei, Jongbloets, Joeri A., van Boxtel, Coco, Hernández, Hugo Pineda, Lips, David, Oliver, Brett G., Hellingwerf, Klaas J., dos Santos, Filipe Branco, 2018b. Alignment of microbial fitness with engineered product formation: obligatory coupling between acetate production and photoautotrophic growth. Biotechnol. Biofuels 11 (1), 38. https://doi.org/10.1186/s13068-018-1037-8.

Ducat, Daniel, Avelar-Rivas, J. Abraham, Way, Jeffrey C., Silver, Pamela A., 2012. Rerouting carbon flux to enhance photosynthetic productivity. Appl. Environ. Microbiol. 78 (8), 2660–2668. https://doi.org/10.1128/AEM.07901-11.

Erdrich, Philipp, Knoop, Henning, Steuer, Ralf, Klamt, Steffen, 2014. Cyanobacterial biofuels: new insights and strain design strategies revealed by computational

modeling. Microb. Cell Factories 13 (1), 128. https://doi.org/10.1186/s12934-014-0128-x.
Etschmann, M.M.W., Bluemke, W., Sell, D., Schrader, J., 2002. Biotechnological production of 2-phenylethanol. Appl. Microbiol. Biotechnol. 59 (1), 1–8. https://doi.org/10.1007/s00253-002-0992-x.
Fang, Ruozhou, Sung, Chih Jen, 2021. A rapid compression machine study of 2-phenylethanol autoignition at low-to-intermediate temperatures. Energies 14 (22). https://doi.org/10.3390/en14227708.
Fernandes, Raquel, Campos, Joana, Serra, Mónica, Fidalgo, Javier, Almeida, Hugo, Casas, Ana, Toubarro, Duarte, Barros, Ana I.R.N.A., 2023. Exploring the benefits of phycocyanin: from *Spirulina* cultivation to its widespread applications. Pharmaceuticals (Basel, Switzerland) 16 (4). https://doi.org/10.3390/ph16040592.
Gao, Zhengxu, Zhao, Hui, Li, Zhimin, Tan, Xiaoming, Lu, Xuefeng, 2012. Photosynthetic production of ethanol from carbon dioxide in genetically engineered cyanobacteria. Energy Environ. Sci. 5 (12), 9857–9865. https://doi.org/10.1039/c2ee22675h.
Gu, Yang, Ma, Jingbo, Zhu, Yonglian, Peng, Xu., 2020. Refactoring Ehrlich pathway for high-yield 2-phenylethanol production in *Yarrowia lipolytica*. ACS Synth. Biol. 9 (3), 623–633. https://doi.org/10.1021/acssynbio.9b00468.
Hamouda, Ragaa A., El-Ahmady El-Naggar, Noura, 2021. Chapter 14 — Cyanobacteria-based microbial cell factories for production of industrial products. In: Vijai, B.T. (Ed.), Microbial Cell Factories Engineering for Production of Biomolecules Singh. Academic Press, pp. 277–302. https://doi.org/10.1016/B978-0-12-821477-0.00007-6.
Hanaoka, Mitsumasa, Takai, Naoki, Hosokawa, Norimune, Fujiwara, Masayuki, Akimoto, Yuki, Kobori, Nami, Iwasaki, Hideo, Kondo, Takao, Tanaka, Kan, 2012. RpaB, another response regulator operating circadian clock-dependent transcriptional regulation in *Synechococcus elongatus* PCC 7942*. J. Biol. Chem. 287 (31), 26321–26327. https://doi.org/10.1074/jbc.M111.338251.
Hays, Stephanie G., Ducat, Daniel C., 2018. Factories. Engineering 123 (3), 285–295. https://doi.org/10.1007/s11120-014-9980-0.
Higashide, Wendy, Li, Yongchao, Yang, Yunfeng, Liao, James C., 2011. Metabolic engineering of *Clostridium cellulolyticum* for production of isobutanol from cellulose. Appl. Environ. Microbiol. 77 (8), 2727–2733. https://doi.org/10.1128/AEM.02454-10.
Hsieh-Lo, Ming, Castillo, Gustavo, Ochoa-Becerra, Mario Alberto, Mojica, Luis, 2019. Phycocyanin and phycoerythrin: strategies to improve production yield and chemical stability. Algal Res. 42, 101600. https://doi.org/10.1016/j.algal.2019.101600.
Jaiswal, Damini, Wangikar, Pramod P., 2020. Dynamic inventory of intermediate metabolites of cyanobacteria in a diurnal cycle. IScience 23 (11), 101704. https://doi.org/10.1016/j.isci.2020.101704.
Kratky, L., Jirout, T., Belohlav, V., 2023. Economic feasibility study for artificial lighting of microalgal flat-panel photobioreactors. Int. J. Environ. Sci. Technol. https://doi.org/10.1007/s13762-023-04804-0.
Kukil, Kateryna, Englund, Elias, Crang, Nick, Hudson, Elton P., Lindberg, Pia, 2023. Laboratory evolution of *Synechocystis* sp. PCC 6803 for phenylpropanoid production. Metab. Eng. 79, 27–37. https://doi.org/10.1016/j.ymben.2023.06.014.
Kwan, Penz Penz, Banerjee, Sanjoy, Shariff, Mohamed, Fatimah, Md., Yusoff., 2021. Influence of light on biomass and lipid production in microalgae cultivation. Aquac. Res. 52 (4), 1337–1347. https://doi.org/10.1111/are.15023.
Labarre, J., Thuriaux, P., Chauvat, F., 1987. Genetic analysis of amino acid transport in the facultatively heterotrophic cyanobacterium *Synechocystis* sp. strain 6803. J. Bacteriol. 169 (10), 4668–4673. https://doi.org/10.1128/jb.169.10.4668-4673.1987.
Levasseur, Wendie, Perré, Patrick, Pozzobon, Victor, 2020. A review of high value-added molecules production by microalgae in light of the classification. Biotechnol. Adv. 41, 107545. https://doi.org/10.1016/j.biotechadv.2020.107545.
Li, Ming, Dawei, Hu, Liu, Hong, 2014. Photobioreactor with ideal light–dark cycle designed and built from mathematical modeling and CFD simulation. Ecol. Eng. 73, 162–167. https://doi.org/10.1016/j.ecoleng.2014.09.010.
Lisondro, Isaac, Serrano, Cintia Gómez, Sepúlveda, Claudia, Ceballos, Ariadna Indira Batista, Fernández, Francisco Gabriel Acién, 2022. Influence of irradiance on the growth and biochemical composition of *Nitzschia* aff. *pellucida*. J. Appl. Phycol. 34 (1), 19–30. https://doi.org/10.1007/s10811-021-02605-x.
Lopes, Graciliana, Clarinha, Duarte, Vasconcelos, Vitor, 2020. Carotenoids from cyanobacteria: a biotechnological approach for the topical treatment of psoriasis. Microorganisms 8 (2). https://doi.org/10.3390/microorganisms8020302.
Luan, Guodong, Zhang, Shanshan, Wang, Min, Lu, Xuefeng, 2019. Progress and perspective on cyanobacterial glycogen metabolism engineering. Biotechnol. Adv. 37 (5), 771–786. https://doi.org/10.1016/j.biotechadv.2019.04.005.
Luimstra, Veerle M., Merijn Schuurmans, J., Verschoor, Antonie M., Hellingwerf, Klaas J., Huisman, Jef, Matthijs, Hans C.P., 2018. Blue light reduces photosynthetic efficiency of cyanobacteria through an imbalance between photosystems I and II. Photosynth. Res. 138 (2), 177–189. https://doi.org/10.1007/s11120-018-0561-5.
Luo, Hu-Ping, Al-Dahhan, Muthanna H., 2011. Verification and validation of CFD simulations for local flow dynamics in a draft tube airlift bioreactor. Chem. Eng. Sci. 66 (5), 907–923. https://doi.org/10.1016/j.ces.2010.11.038.
Luo, Xiao, Li, Jiaxing, Chang, Tianliang, He, Hongyan, Zhao, Yi, Yang, Xue, Zhao, Yuwei, Xu, Yao, 2019. Stable reference gene selection for RT-QPCR analysis in *Synechococcus elongatus* PCC 7942 under abiotic stresses. In: El-Matbouli, Mansour (Ed.), BioMed Research International 2019, p. 7630601. https://doi.org/10.1155/2019/7630601.
Mahlmann, Daniel M., Jahnke, Joachim, Loosen, Peter, 2008. Rapid determination of the dry weight of single, living cyanobacterial cells using the Mach-Zehnder double-beam interference microscope. Eur. J. Phycol. 43 (4), 355–364. https://doi.org/10.1080/09670260802168625.
Maltsev, Yevhen, Maltseva, Kateryna, Kulikovskiy, Maxim, Maltseva, Svetlana, 2021. Influence of light conditions on microalgae growth and content of lipids, carotenoids, and fatty acid composition. Biology 10 (10). https://doi.org/10.3390/biology10101060.
Mannino, Giuseppe, Iovino, Piera, Lauria, Antonino, Genova, Tullio, Asteggiano, Alberto, Notarbartolo, Monica, Porcu, Alessandra, et al., 2021. Bioactive triterpenes of protium heptaphyllum gum resin extract display cholesterol-lowering potential. Int. J. Mol. Sci. 22 (5). https://doi.org/10.3390/ijms22052664.
Martínez-Avila, Oscar, Sánchez, Antoni, Font, Xavier, Barrena, Raquel, 2018. Bioprocesses for 2-phenylethanol and 2-phenylethyl acetate production: current state and perspectives. Appl. Microbiol. Biotechnol. 102 (23), 9991–10004. https://doi.org/10.1007/s00253-018-9384-8.
Masojídek, Jiří, Torzillo, Giuseppe, Koblížek, Michal, 2013. Photosynthesis in microalgae. In: Handbook of Microalgal Culture, pp. 21–36. https://doi.org/10.1002/9781118567166.ch2.
Masuo, Shunsuke, 2024. Microbial production of aromatic compounds and synthesis of high-performance bioplastics. Biosci. Biotechnol. Biochem. https://doi.org/10.1093/bbb/zbae111.
Mir, Rafia, Jallu, Shais, Singh, T.P., 2015. The shikimate pathway: review of amino acid sequence, function and three-dimensional structures of the enzymes. Crit. Rev. Microbiol. 41 (2), 172–189. https://doi.org/10.3109/1040841X.2013.813901.
Nedbal, Ladislav, Trtílek, Martin, Cervený, Jan, Komárek, Ondrej, Pakrasi, Himadri B., 2008. A photobioreactor system for precision cultivation of photoautotrophic microorganisms and for high-content analysis of suspension dynamics. Biotechnol. Bioeng. 100 (5), 902–910. https://doi.org/10.1002/bit.21833.
Ni, Jun, Liu, Hong Yu, Tao, Fei, Wu, Yu Tong, Xu, Ping, 2018. Remodeling of the photosynthetic chain promotes direct CO_2 conversion into valuable aromatic compounds. Angew. Chem. Int. Ed. 57 (49), 15990–15994. https://doi.org/10.1002/anie.201808402.
Noda, Shuhei, Mori, Yutaro, Ogawa, Yuki, Fujiwara, Ryosuke, Dainin, Mayumi, Shirai, Tomokazu, Kondo, Akihiko, 2024. Metabolic and enzymatic engineering approach for the production of 2-phenylethanol in engineered *Escherichia coli*. Bioresour. Technol. 406, 130927. https://doi.org/10.1016/j.biortech.2024.130927.
Nogales, Juan, Gudmundsson, Steinn, Knight, Eric M., Palsson, Bernhard O., Thiele, Ines, 2012. Detailing the optimality of photosynthesis in cyanobacteria through systems biology analysis. Proc. Natl. Acad. Sci. 109 (7), 2678–2683. https://doi.org/10.1073/pnas.1117907109.
Oliveira, Paulo, Lindblad, Peter, 2011. Novel insights into the regulation of LexA in the cyanobacterium *Synechocystis* sp. strain PCC 6803. J. Bacteriol. 193 (15), 3804–3814. https://doi.org/10.1128/JB.00289-11.
Pérez, Adam A., Chen, Que, Hernández, Hugo Pineda, Santos, Filipe Branco Dos, Hellingwerf, Klaas J., 2019. On the use of oxygenic photosynthesis for the sustainable production of commodity chemicals. Physiol. Plant. 166 (1), 413–427. https://doi.org/10.1111/ppl.12946.
Pleonsil, Pornthip, Soogarun, Suphan, Suwanwong, Yaneenart, 2013. Anti-oxidant activity of Holo- and Apo-c-phycocyanin and their protective effects on human erythrocytes. Int. J. Biol. Macromol. 60 (September), 393–398. https://doi.org/10.1016/j.ijbiomac.2013.06.016.
Rahman, Mizanur, Asaeda, Takashi, Abeynayaka, Helayaye Damitha Lakmali, Fukahori, Kiyotaka, 2023. An assessment of the effects of light intensities and temperature changes on cyanobacteria's oxidative stress via the use of hydrogen peroxide as an indicator. Water 15 (13). https://doi.org/10.3390/w15132429.
Savakis, Philipp E., Andreas Angermayr, S., Hellingwerf, Klaas J., 2013. Synthesis of 2,3-butanediol by *Synechocystis* sp. PCC6803 via heterologous expression of a catabolic pathway from lactic acid- and enterobacteria. Metab. Eng. 20, 121–130. https://doi.org/10.1016/j.ymben.2013.09.008.
Schuurmans, R. Milou, van Alphen, Pascal, Schuurmans, J. Merijn, Matthijs, Hans C.P., Hellingwerf, Klaas J., 2015. Comparison of the photosynthetic yield of cyanobacteria and green algae: different methods give different answers. PLoS One 10 (9), e0139061. https://doi.org/10.1371/journal.pone.0139061.
Severinghaus, J.W., Bradley, A.F., 1958. Electrodes for blood PO_2 and PCO_2 determination. J. Appl. Physiol. 13 (3), 515–520. https://doi.org/10.1152/jappl.1958.13.3.515.
Sforza, Eleonora, Barbera, Elena, Bertucco, Alberto, 2015. Improving the photoconversion efficiency: an integrated photovoltaic-photobioreactor system for microalgal cultivation. Algal Res. 10, 202–209. https://doi.org/10.1016/j.algal.2015.05.005.
da Silva Ferreira, Veronica, Sant'Anna, Celso, 2016. Impact of culture conditions on the chlorophyll content of microalgae for biotechnological applications. World J. Microbiol. Biotechnol. 33 (1), 20. https://doi.org/10.1007/s11274-016-2181-6.
Singh, Vishal, Mishra, Vishal, 2023. A review on the current application of light-emitting diodes for microalgae cultivation and its fiscal analysis. Crit. Rev. Biotechnol. 43 (5), 665–679. https://doi.org/10.1080/07388551.2022.2057274.
Sobolewska, Ewelina, Borowski, Sebastian, Nowicka-Krawczyk, Paulina, 2023. Effect of solar and artificial lighting on microalgae cultivation and treatment of liquid digestate. J. Environ. Manag. 344, 118445. https://doi.org/10.1016/j.jenvman.2023.118445.
Solimeno, Alessandro, Samsó, Roger, Uggetti, Enrica, Sialve, Bruno, Steyer, Jean-Philippe, Gabarró, Adrián, García, Joan, 2015. New mechanistic model to simulate microalgae growth. Algal Res. 12, 350–358. https://doi.org/10.1016/j.algal.2015.09.008.
Soman, Abhinav, Shastri, Yogendra, 2015. Optimization of novel photobioreactor design using computational fluid dynamics. Appl. Energy 140, 246–255. https://doi.org/10.1016/j.apenergy.2014.11.072.

Szwarc, Dawid, Zieliński, Marcin, 2018. Effect of lighting on the intensification of phycocyanin production in a culture of *Arthrospira platensis*. Proceedings. https://doi.org/10.3390/proceedings2201305.

Tamburic, Bojan, Evenhuis, Christian R., Crosswell, Joseph R., Ralph, Peter J., 2018. An empirical process model to predict microalgal carbon fixation rates in photobioreactors. Algal Res. 31, 334–346. https://doi.org/10.1016/j.algal.2018.02.014.

Usai, Giulia, Cordara, Alessandro, Re, Angela, Polli, Maria Francesca, Mannino, Giuseppe, Bertea, Cinzia Margherita, Fino, Debora, Pirri, Candido Fabrizio, Menin, Barbara, 2022. Combining metabolite doping and metabolic engineering to improve 2-phenylethanol production by engineered cyanobacteria. Front. Bioeng. Biotechnol. 10 (September), 1–18. https://doi.org/10.3389/fbioe.2022.1005960.

Usai, Giulia, Cordara, Alessandro, Mazzocchi, Elena, Re, Angela, Fino, Debora, Pirri, Candido Fabrizio, Menin, Barbara, 2024. Coupling dairy wastewaters for nutritional balancing and water recycling: sustainable heterologous 2-phenylethanol production by engineered cyanobacteria. Front. Bioeng. Biotechnol. 12. https://doi.org/10.3389/fbioe.2024.1359032.

Vasile, Nicolò S., Cordara, Alessandro, Usai, Giulia, Re, Angela, 2021. Computational analysis of dynamic light exposure of unicellular algal cells in a flat-panel photobioreactor to support light-induced CO_2 bioprocess development. Front. Microbiol. 12, 579. https://doi.org/10.3389/fmicb.2021.639482.

Wellburn, Alan R., 1994. The spectral determination of chlorophylls a and b, as well as total carotenoids, using various solvents with spectrophotometers of different resolution. J. Plant Physiol. 144 (3), 307–313. https://doi.org/10.1016/S0176-1617(11)81192-2.

Yen, Hong-Wei, Ho, Shih-Hsin, Chen, Chun-Yen, Chang, Jo-Shu, 2015. CO_2, NO_x and SO_x removal from flue gas via microalgae cultivation: a critical review. Biotechnol. J. 10 (6), 829–839. https://doi.org/10.1002/biot.201400707.

Zavřel, Tomáš, Chmelík, Dominik, Sinetova, Maria A., Červený, Jan, 2018. Spectrophotometric determination of phycobiliprotein content in cyanobacterium *Synechocystis*. J. Visual. Exp. 139 (September). https://doi.org/10.3791/58076.

Zhang, Dongda, Dechatiwongse, Pongsathorn, Hellgardt, Klaus, 2015. Modelling light transmission, cyanobacterial growth kinetics and fluid dynamics in a laboratory scale multiphase photo-bioreactor for biological hydrogen production. Algal Res. 8, 99–107. https://doi.org/10.1016/j.algal.2015.01.006.

Zhang, Zhibo, Wang, Yaowei, Zhang, Dongrui, Zhao, Deming, Shi, Huibin, Yan, Hao, Zhou, Xin, Feng, Xiang, Yang, Chaohe, 2024. Integration of physical information and reaction mechanism data for surrogate prediction model and multi-objective optimization of glycolic acid production. Green Chem. Eng. https://doi.org/10.1016/j.gce.2024.06.002.

Zhu, Chenghui, Ling, Qinjie, Cai, Zhihui, Wang, Yun, Zhang, Yibo, Hoffmann, Peter R., Zheng, Wenjie, Zhou, Tianhong, Huang, Zhi, 2016. Selenium-containing phycocyanin from Se-enriched *Spirulina platensis* reduces inflammation in dextran sulfate sodium-induced colitis by inhibiting NF-κB activation. J. Agric. Food Chem. 64 (24), 5060–5070. https://doi.org/10.1021/acs.jafc.6b01308.

Zieliński, Marcin, Dębowski, Marcin, Kazimierowicz, Joanna, Świca, Izabela, 2023. Microalgal carbon dioxide (CO_2) capture and utilization from the European Union perspective. Energies 16 (3), 1–27. https://doi.org/10.3390/en16031446.